

On the choice of the mesh for the analysis of geostatistical data using R-INLA

Peer-reviewed author version

RIGHETTO, Ana; FAES, Christel; VANDENDIJCK, Yannick & Ribeiro Jr, Paulo Justiniano (2020) On the choice of the mesh for the analysis of geostatistical data using R-INLA. In: COMMUNICATIONS IN STATISTICS-THEORY AND METHODS, 49 (1) , p. 203 -220.

DOI: 10.1080/03610926.2018.1536209

Handle: <http://hdl.handle.net/1942/30576>

# On the choice of the mesh for the analysis of geostatistical data using R-INLA

**Ana Julia Righetto**

Departamento de Ciências Exatas,  
Universidade de São Paulo,  
13418-900, Piracicaba, SP, Brazil.

e-mail: *ajrighetto@gmail.com* (corresponding author)

**Christel Faes and Yannick Vandendijck**

Interuniversity Institute for Biostatistics and  
statistical Bioinformatics (I-BioStat),  
Hasselt University, Hasselt, Belgium

e-mail: *christel.faes@uhasselt.be* and *yannick.vandendijck@uhasselt.be*

**Paulo Justiniano Ribeiro Junior**

Departamento de Estatística,  
Universidade Federal do Paraná, Brazil

e-mail: *paulojus@ufpr.br*

## Abstract

Many methods used in spatial statistics are computationally demanding, and so, the development of more computationally efficient methods has received attention. A important development is the integrated nested Laplace approximation method which is carry out Bayesian analysis more efficiently This method, for geostatistical data, is done considering the SPDE approach that requires the creation of a mesh overlying the study area and all the obtained results depend on it. The impact of the mesh on inference and prediction is investigated through simulations. As there is no formal procedure to specify it, we investigate a guideline to create an optimal mesh

*Keywords:* Geostatistics; Integrated nested Laplace approximation; Mesh; Stochastic partial differential equation;

## 1 Introduction

Models in spatial statistics are used to measure properties and relationships of a geographically measured outcome, explicitly taking into account the spatial locations of the studied phenomenon. Traditional methods in spatial statistics were developed without the consideration of computational efficiency, as in many applications the sample size was limited due to the cost involved in obtaining the measurements (Bolin and Lindgren, 2013). Nowadays, however, with the increasing use of geographic information systems and global positioning systems, large data sets are becoming available, and computational efficiency has become extremely important.

Geostatistical data are widely analyzed using the kriging method, an optimal interpolation method employing the spatial autocorrelation to derive predictions at unmeasured locations (Gelfand et al., 2010). A popular choice to estimate the statistical dependence is the Matérn family of covariance functions, which includes, for example, the exponential and Gaussian covariance functions, as particular cases. For inference, it is common to use the Bayesian framework,

which is based on the observed data only and easily allows for sequential updating of information. Sampling methods such as Markov Chain Monte Carlo (MCMC) are well known in Bayesian inference, but demand intense computation time.

As an alternative to the computational intensive MCMC methods, Rue, Martino and Chopin (2009) proposed the use of integrated nested Laplace approximations (INLA). INLA is an approximate method designed for inference of latent Gaussian models, a very wide and flexible class of models ranging from (generalized) linear mixed model to spatial and spatio-temporal models (Lindgren and Rue, 2015). When combined with stochastic partial differential equation (SPDE) (Lindgren, Rue and Lindstrom, 2011), it can accommodate georeferenced data from all sub-areas of spatial statistics (geostatistics, lattice data and point processes). Recently, INLA has received considerable attention due to its accuracy and computational speed (Karagiannis et al., 2013; Lindgren, 2012).

The SPDE approach approximates the Gaussian field using a Gaussian Markov random field. For geostatistical data, the spatial field is described using a weighted sum of piece-wise linear basis function that is usually defined from a triangularization of the study area, called the mesh. The accuracy of the estimates as well as the predictions will depend on the mesh specification. The idea is that smaller triangles will increase the accuracy, though when the spatial range is larger, larger triangles can be used. The mesh can be constructed using different principles. A common method, using R-INLA, is to use the locations of the measurements as initial triangulation vertices, and add or remove knots according to the size for the edges of the triangles of the inside mesh (which includes the study region), for the edges of the outer mesh (outside the study area, to avoid border effects) and to the shortest distance allowed between the junctions of the edges (knots). Each combination of these three values implies a certain number of knots on the mesh, and more knots can increase in the computational cost. While it has been indicated that the choice of the mesh must be done carefully (Lindgren and Rue, 2015), no conclusive way to create the best mesh has been described.

As the analysis depends on the chosen mesh, the objective of this work is to extensively study the parameters for the creation of the mesh, to see their impact on the analysis and set guidelines to construct the optimal mesh in two dimensional spatial domains, for irregular geostatistical data, solving some issues raised by Bolin and Lindstrom (2014). In Section 2, we give a brief introduction to INLA and the SPDE approach and discuss some criteria to evaluate the mesh. A simulation study is performed in Section 2.3 and an application with real data set is provided in Section 4. A discussion is provided in Section 5.

## 2 INLA and SPDE

INLA is a deterministic method to perform Bayesian inference of latent Gaussian models, avoiding computational intensive Markov chain Monte Carlo simulations (Rue, Martino and Chopin, 2009). The method is designed for a large class of Gaussian Markov random fields (GMRF), including many of the hierarchical models with latent Gaussian processes. If  $\mathbf{y}$  represents the data,  $\mathbf{x}$  the GMRF and  $\boldsymbol{\theta}$  the vector of hyperparameters, the idea of INLA is to approximate the posterior density  $\Pi(\boldsymbol{\theta}|\mathbf{y})$  via Gaussian approximation of the posterior of the latent field  $\Pi(\mathbf{x}|\boldsymbol{\theta}, \mathbf{y})$  and a Laplace approximation in the latent field marginal posterior calculations. Details can be found in Rue, Martino and Chopin (2009).

Lindgren, Rue and Lindstrom (2011) showed that the use of INLA is not restricted to discrete spatial domains, given there is a connection between continuous domains and Markov models. Indeed, a large class of random field models can be expressed as a solution of a continuous domains stochastic partial differential equation (SPDE). Whittle (1954) showed that the Matérn covariance function can be seen as a solution of the SPDE. The Matérn function is given by  $M(\mathbf{h}|k, \phi) = \frac{2^{1-k}}{\Gamma(k)} (\phi \|\mathbf{h}\|)^k K_k(\phi \|\mathbf{h}\|)$ , in which  $\Gamma(\cdot)$  is the Gamma function,  $K_k$  is Bessel function with order  $k$  and  $\|\mathbf{h}\|$  is the distance between two locations. This connection allows one to carry out the calculations for a continuous random field using the (discrete) GMRF representation.

This is done by approximating the spatial field as a basis function representation:

$$\mathbf{x}(s) = \sum_{k=1}^K \Psi_k(s) \mathbf{x}_k, \quad (1)$$

where  $\Psi_k(s)$  are piece-wise linear basis function defined on a triangulation of the study domain and  $\{\mathbf{x}_1, \dots, \mathbf{x}_K\}$  are Gaussian weights chosen to approximate the solutions to the SPDE on the domain. The triangulation consists in subdividing the study area into a set of non-intersecting triangles (Cameletti et al., 2012), with linear basis function defined with barycentric interpolation. This SPDE/GMRF analysis is available in the R-package INLA (Rue, Martino and Chopin, 2009).

The first step of the analysis is the construction of a triangulated mesh on which the SPDE/GMRF representation is built (Lindgren, 2012). As an initial step, we can choose to place the triangle vertices at the locations where measurements were taken, and after that, add or remove additional vertices, creating the triangulation for the analysis. As the solution may present a border effect, it is necessary to extend the mesh also outside the study area to avoid it. According to Lindgren (2012), the effect in constructing triangles is that we can obtain small ones (and so obtain high accuracy to represent the field) where the locations are dense, and bigger ones when the locations are sparse. As the analysis depends on the mesh, it is very important to create a mesh suited for the data at hand.

In the R-INLA implementation, the functions `inla.mesh.1d` and `inla.mesh.2d()` are available to create the mesh. The function `inla.mesh.1d` is used to define B-spline basis representations in one dimension (Lindgren and Rue, 2015) and has less parametrization than the `inla.mesh.2d()`, which is used for representations in two dimension and has several parameters that can be chosen as to construct a mesh for the problem at hand, e.g. the `max.edge` parameters define the maximal allowed lengths of triangle edges in the inner domain and in the outer extension, the `cutoff` parameter corresponds with the shortest distance allowed between points (Krainski and Lindgren, 2014; Krainski and Rue, 2013). A change in one of these values, will create a different mesh, making it more or less dense (with more or less knots). The focus of this paper is to work with the function `inla.mesh.2d()`, which is the one widely used for geostatistical data set.

We will work with the above three arguments for building the convex mesh: the maximal allowed edge length in the inner domain ( $a$ ) and outer domain ( $b$ ), and the shortest allowed distance between points ( $c$ ). We will always consider larger values of the maximal allowed edge length for the outer domain as for the inner domain ( $b > a$ ), as the outer domain is needed only to avoid border effects.

For exploratory reasons, we illustrated how the choice of these parameters determine the aspect of the mesh in Figure 1. We consider 100 randomly generated locations of a spatial process on the unit square. Starting with these locations as initial vertices of the triangulation, we create different meshes, depending on the parameters  $a$ ,  $b$  and  $c$ . In the left panel, we fix the maximal allowed edge length ( $b = 0.4$ ) and shortest distance allowed between points ( $c = 0.001$ ), but change the value of the maximal allowed edge length in the inner domain ( $a = (0.03, 0.07, 0.11)$ ). By increasing the maximal allowed edge length, the triangulation becomes less dense, with the number of vertices decreasing from 3737 to 781 and 417, respectively. The right panel in Figure 1 shows the impact of increasing the minimal allowed distance between vertices ( $c = 0.01, 0.03, 0.06$ ). The edge length for the inner and outer domain was kept fix ( $a = 0.07, b = 0.4$ ). While changing  $c$  from 0.001 (panel II) to 0.01 (panel IV) has only little impact, a further increase of  $c$  has a bigger one, changing the number of vertices to 774, 765 and 299, respectively. By increasing the value of  $c$ , less clustered vertices are observed, making the mesh more regular over the whole domain. Even a small change in one parameter to construct the mesh can generate a complete different mesh and the results will be affected. Then, the focus of this survey is to investigate the impact of the mesh in the analysis.

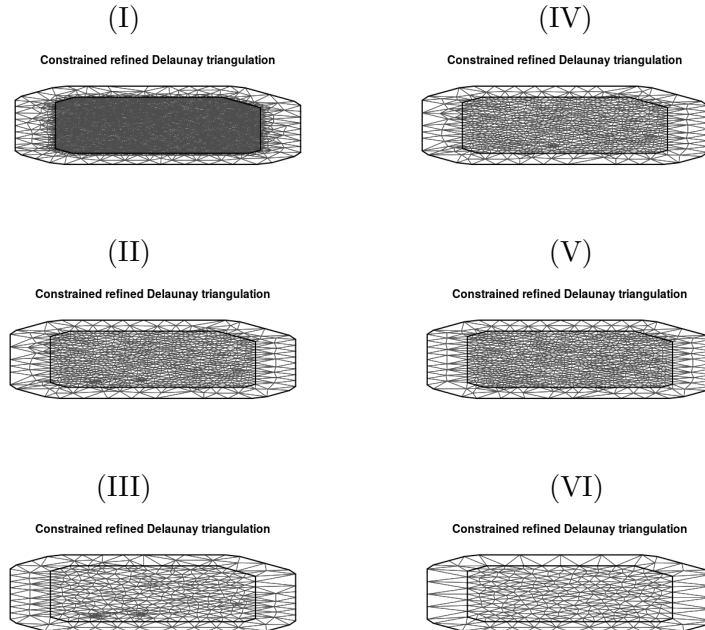


Figure 1: Example of meshes with  $b = 0.40$  and  $(a, c)$  given by (I) (0.03, 0.001), (II) (0.07, 0.001), (III) (0.11, 0.001), (IV) (0.07, 0.01), (V) (0.07, 0.03), (VI) (0.07, 0.06)

## 2.1 Model fitting and predictive information criteria

To evaluate and compare the performance of different meshes, different predictive information criteria can be used. Three information criteria are considered in this study: the deviance information criterion (DIC), the Watanabe-Akaike information criterion (WAIC) and the conditional predictive ordinate (CPO). In Section 3.3, we investigate the performance of these criteria to perform mesh selection. These criteria are briefly explained below.

The deviance information criterion, described by Spiegelhalter et al. (2000), is defined as

$$DIC = -2 \log p(\mathbf{y}|\hat{\boldsymbol{\theta}}) + 2p_{DIC},$$

where  $2 \log p(\mathbf{y}|\hat{\boldsymbol{\theta}})$  is the posterior expected deviance measuring the suitability of the model,  $p_{DIC}$  the estimated effective number of parameters of the model, representing the complexity of the model and  $\hat{\boldsymbol{\theta}}$  is the expectation of  $\boldsymbol{\theta}$ . In this way, DIC takes into consideration both the suitability and complexity of the model.

Proposed by Watanabe (2010), WAIC can be viewed as an improvement on the DIC for Bayesian models (Vehtari and Gelman, 2014) and is given by

$$WAIC = -2 \log \int p(\mathbf{y}|\boldsymbol{\theta})\Pi(\boldsymbol{\theta}|\mathbf{y})d\boldsymbol{\theta} + \sum_{i=1}^n Var(\log(p(y_i|\boldsymbol{\theta}))).$$

Similar as with DIC, the first term measures the predictive performance, and the second term penalizes for model complexity. Compared to DIC, WAIC averages  $p(\mathbf{y}|\boldsymbol{\theta})$  over the posterior distribution of  $\boldsymbol{\theta}$ , whereas DIC conditions on the point estimate of  $\boldsymbol{\theta}$ . The complexity term is a sum of the variance for each data point separately, yielding more stable results as DIC (Gelman, Hwang and Vehtari, 2014).

The conditional predictive ordinate is a cross-validation method, estimating the leave-one-out predictive distribution (Geisser and Eddy, 1979). The posterior predictive distribution for an observation  $i$  can be expressed as

$$p(\mathbf{y}_i|\mathbf{y}_{-i}) = \int p(\mathbf{y}_i|\boldsymbol{\theta})\Pi(\boldsymbol{\theta}|\mathbf{y}_{-i})d\boldsymbol{\theta},$$

where  $\mathbf{y}_i$  is the  $i$ th observation of  $\mathbf{y}$  and  $\mathbf{y}_{-i}$  is  $\mathbf{y}$  without observation  $i$ . So the CPO is the probability a posteriori to observe  $y_i$  when the model is adjusted without  $y_i$ . A bigger value of CPO indicates a better adjustment. Instead of having to refit the model each time, an approximation of CPO can be obtained by sampling from the posterior distribution:

$$CPO_i = \frac{1}{T^{-1} \sum_{t=1}^T p(\mathbf{y}_i | \boldsymbol{\theta}^t)^{-1}},$$

where  $\boldsymbol{\theta}^t$  is a sample from  $\Pi(\boldsymbol{\theta} | y_i)$  and  $T$  indicated the number of posterior samples. This is the inverse of the posterior mean of the inverses of the likelihood. This is an efficient method, but requires care since numerical problems in the calculations can occur (Held, Schrodle and Rue, 2010). However, when using INLA it is possible to verify if numerical problems did occur and recompute the CPO using a less efficient method (re-fitting the model for every observation).

In this work we used a summary by calculating the log-score, given by

$$\log CPO = -\frac{1}{n} \sum_{i=1}^n \log(p(\mathbf{y}_i | \mathbf{y}_{-i})).$$

This log-score is an estimator of the log marginal likelihood function and smaller values indicate better model performance. In contrast to DIC and WAIC, the log *CPO* score does not adjust for the complexity of the model.

### 3 Simulation Study

In this section, we first describe the simulation design, after which results are discussed. The first goal of the simulation study is to investigate the impact of the choice of the mesh on the inference (parameter estimation and prediction). The second goal is to investigate how we can select an optimal mesh for a particular data problem at hand.

#### 3.1 Simulation Design

A simulation study, with 200 simulation runs, was set up to compare different meshes. Different simulation scenarios are considered. Spatial geostatistical processes with sample sizes of  $n = 300, 100$  and  $50$  are generated. Observed locations are randomly generated on the unit square. A response vector  $\mathbf{y}$  is generated according to the model  $\mathbf{y} = \beta_0 + \beta_1 \mathbf{x} + \mathbf{s} + \mathbf{e}$ , where  $\mathbf{x}$  is a uniformly distributed covariate,  $\mathbf{s}$  is a Matérn spatial random field with correlation function given by  $M(\mathbf{h} | k, \phi) = \frac{1}{2^{k-1} \Gamma(k)} (\phi \|\mathbf{h}\|)^k K_k(\phi \|\mathbf{h}\|)$  and  $\mathbf{e}$  is white noise. Parameters are fixed to  $\beta_0 = 1$ ,  $\beta_1 = 2$ . The spatial variability of the Matérn spatial random field is set to  $\sigma_s^2 = 0.7$  and Gaussian white noise variability to  $\sigma_e^2 = 0.3$ . The nominal range of the spatial random field is specified as  $\phi^* = \frac{\sqrt{8(\alpha - \frac{d}{2})}}{k} = 0.20$ , by setting the smooth parameter  $k = 10$ , the fractional operator order  $\alpha = 1.5$  and  $d = 2$ , as the study region  $\mathbf{A} \in \mathbb{R}^d$ . Note that the choice of  $\alpha = 1.5$  in the Matérn spatial random field corresponds to an exponential random field (Gelfand et al., 2010). For the prior, we used the log-gamma distribution with parameters  $c(1.0, 0.00005)$ . To prevent effects caused by a single choice of coordinates, we conduct the simulation in five batches of 40 simulations and within one batch the coordinates are kept fixed.

To investigate the impact of meshes, different meshes are constructed for the generated processes. The initial triangulation taken is given by the locations of the generated process. Note that, as we keep the coordinates fixed within batches, also the meshes will remain the same within a batch. Different meshes are considered by allowing the `max.edge=(a,b)` and `cutoff=c` parameters to change. The set of values considered for the maximal allowed edge length in the inner domain is  $a = (0.05, 0.09, 0.13, 0.17, 0.19, 0.20)$ , for the maximal edge length in the outer domain is  $b = (0.4, 0.3, 0.2)$  and for the shortest allowed distance between two points is  $c = (0.001, 0.005, 0.01, 0.03, 0.05, 0.07, 0.10, 0.13)$ . Combinations of these three values leads to a total of 144 different meshes. These values were chosen such that the value of  $a$  is smaller or

equal to the range  $\phi^*$ , and the value of  $b$ , controlling the outer boundaries to avoid boundary effects, should be larger than  $a$ . The results are shown for  $b = 0.3$ , as we notice that there is almost no impact for the different values of  $b$

Table 1 summarizes, for the different combination of the parameters  $a$  and  $c$ , the average number of vertices (rounded to integer) in the mesh, for a sample size of  $n = 100$  and a maximal edge length in the outer domain of  $b = 0.3$ . A more dense triangulation is obtained with smaller values of both  $a$  and  $c$ . When the `cutoff` parameter ( $c$ ) is large, the number of vertices in the triangulation is lower than the number of observed locations. In addition, we observe that the influence of  $a$  decreases as  $c$  increases. Results in the next sections focus on the scenario of a sample size of  $n = 100$ . Results for  $n = 50$  and  $n = 300$  are given in the Supplementary Material.

Table 1: Average number of knots for different combinations of the parameters  $a$  and  $c$ , with parameter  $b = 0.3$  and sample size  $n = 100$ .

	<b>c=0.001</b>	<b>c=0.005</b>	<b>c=0.01</b>	<b>c=0.03</b>	<b>c=0.05</b>	<b>c=0.07</b>	<b>c=0.10</b>	<b>c=0.13</b>
<b>a=0.05</b>	1398	1394	1390	989	400	208	120	86
<b>a=0.09</b>	523	517	507	487	400	206	117	84
<b>a=0.13</b>	315	307	293	251	236	206	116	84
<b>a=0.17</b>	272	265	250	203	174	159	115	84
<b>a=0.19</b>	266	259	243	192	160	145	115	84
<b>a=0.20</b>	263	256	241	189	155	140	113	84

### 3.2 Impact of mesh on inference

To investigate the impact of the mesh on the inference, we calculated, for each mesh, the coverage (based on the 95% Confidence Interval), bias and mean squared error (MSE) for each of the parameters in the model and for the predictions.

Table 2 summarizes the simulation coverage for the covariance function parameters ( $\sigma_e^2$ ,  $\sigma_s^2$ ,  $k$  and  $\phi^*$ ) and for  $\beta_0$  and  $\beta_1$ , for meshes with varying maximal allowed edge length in the inner domain ( $a$ ) and varying shortest allowed distance between points ( $c$ ), but with fixed maximal length in the external area (namely,  $b = 0.3$ ). Figure S.1 in the Supplementary Material shows the coverage for all considered meshes.

Table 2: Coverage, in %, of the 95% credible intervals of the parameters  $\beta_0$ ,  $\beta_1$ ,  $\sigma_e^2$ ,  $\sigma_s^2$ ,  $k$  and  $\phi^*$  for different meshes with  $b = 0.3$ .

Mesh	$c$	$a$	Coverage in % for:						Mesh	$c$	$a$	Coverage in % for:					
			$\beta_0$	$\beta_1$	$\sigma_e^2$	$\sigma_s^2$	$k$	$\phi^*$				$\beta_0$	$\beta_1$	$\sigma_e^2$	$\sigma_s^2$	$k$	$\phi^*$
1	0.001	0.05	90.50	90.00	13.50	52.50	30.00	30.00	25	0.05	0.05	97.50	91.00	83.50	96.00	91.00	91.00
2		0.09	92.50	90.00	8.50	17.50	21.50	21.50	26		0.09	98.50	92.00	80.50	96.00	90.00	90.00
3		0.13	93.00	90.50	6.50	9.00	19.00	19.00	27		0.13	99.50	92.50	74.00	97.50	89.50	89.50
4		0.17	92.50	90.00	6.50	8.00	21.00	21.00	28		0.17	99.50	93.00	66.00	97.50	88.50	88.50
5		0.19	92.50	90.50	8.00	9.00	21.50	21.50	29		0.19	99.50	93.00	67.00	96.00	88.00	88.00
6		0.20	92.00	90.00	7.50	8.50	21.50	21.00	30		0.20	99.00	93.50	65.50	96.00	88.50	88.50
7	0.005	0.05	88.50	85.00	17.00	56.50	34.00	34.00	31	0.07	0.05	99.00	92.50	60.50	96.00	87.00	86.50
8		0.09	89.50	84.00	13.00	26.50	26.00	26.00	32		0.09	99.50	92.00	59.00	95.50	86.50	86.50
9		0.13	89.50	84.00	12.00	16.00	25.50	25.50	33		0.13	99.50	92.50	59.50	95.50	86.50	86.50
10		0.17	89.50	84.00	12.00	16.00	27.00	27.00	34		0.17	99.00	94.00	44.00	94.50	82.00	82.00
11		0.19	89.00	84.50	12.00	15.00	26.50	26.50	35		0.19	99.00	92.50	39.50	96.00	85.00	85.00
12		0.20	88.50	84.50	12.50	15.50	26.50	26.00	36		0.20	99.50	92.50	36.50	96.50	84.00	84.00
13	0.01	0.05	92.00	86.00	36.50	70.50	52.00	52.00	37	0.10	0.05	99.50	93.50	20.50	93.50	83.50	83.50
14		0.09	94.00	90.00	38.50	50.00	48.50	48.50	38		0.09	99.50	92.50	19.50	92.50	82.00	82.00
15		0.13	92.50	89.50	37.50	39.50	46.50	46.50	39		0.13	99.50	93.50	19.00	93.50	82.50	82.50
16		0.17	92.50	89.00	39.00	38.00	47.00	47.00	40		0.17	99.50	93.50	19.50	93.00	84.00	84.00
17		0.19	92.50	89.00	37.00	37.00	48.00	48.50	41		0.19	99.50	93.50	19.50	92.50	85.00	85.00
18		0.20	92.00	89.00	37.50	37.50	48.50	48.00	42		0.20	99.50	93.00	18.50	93.00	85.50	85.50
19	0.03	0.05	95.50	90.00	79.00	91.00	89.50	88.50	43	0.13	0.05	98.50	93.50	2.50	94.50	86.00	86.00
20		0.09	97.00	92.00	83.50	94.00	92.50	92.50	44		0.09	98.50	93.00	2.00	94.50	89.00	89.00
21		0.13	98.00	92.50	81.50	94.00	91.50	92.00	45		0.13	98.50	93.50	3.00	94.00	89.50	90.00
22		0.17	98.00	93.50	80.50	92.00	89.50	90.00	46		0.17	98.50	93.50	3.00	94.00	89.50	90.00
23		0.19	97.50	94.00	78.00	90.50	90.00	90.50	47		0.19	98.50	93.00	3.00	94.00	89.50	90.50
24		0.20	97.50	94.00	78.50	91.00	90.50	90.50	48		0.20	98.50	93.50	3.00	94.50	89.50	90.00

It can be observed that the largest impact on the coverage is observed for the `cutoff` parameter  $c$ . The parameters  $\beta_0$  and  $\beta_1$  have good coverage specially for meshes with high values of  $c$ .

Increasing the shortest allowed distance, improves the coverage for the parameters  $\sigma_s^2$ ,  $k$  and  $\phi^*$ , no matter much the value of  $a$ . However, we also observe an undercoverage for the parameter  $\sigma_e^2$ , especially if  $c$  gets too small or too large. Overall, we can also observe that an increase of the maximal allowed edge length in the inner domain ( $a$ ) has a negative impact on the coverage of most parameters. These results show that, indeed, the choice of the mesh is very important to obtain good coverage for the covariance parameters. Mesh 20, with  $a = 0.09$ ,  $b = 0.3$  and  $c = 0.03$ , has the best coverage of  $\sigma_e^2$ ,  $k$  and  $\phi^*$ , meshes 27 and 28 have the best results for  $\sigma_s^2$  and meshes with  $c = 0.10$  have the best coverage for  $\beta_0$  and  $\beta_1$ . So there does not seem to be one mesh that is outperforming all other meshes for all parameters together. Considering the coverage of all parameters together, mesh 20 has the best results overall.

Results given in the Supplementary Material with sample size of  $n = 50$  or  $n = 300$  are very similar (see Figures S.2 and S.3 and Tables S.1 and S.2 of Supplementary Material). When the value of the `cutoff` parameter  $c$  is very small, the coverage for all covariance parameters is too low. Increasing the value of  $c$ , decreases the number of knots in the mesh, but leads to better nominal coverages. However, when  $c$  is too large, the coverage for  $\sigma_e^2$  drops again. The impact of changing the maximal allowed length in the inner domain ( $a$ ) has much less impact on the nominal coverage and changing the value of  $b$ , the maximal allowed length in the outer domain, has no impact. The mesh with best coverage depends on the parameter of interest and the sample size: for  $\sigma_e^2$ , mesh 29 has a slightly better results for coverage when  $n = 50$  and for all the others parameters, mesh 45 is outstanding when  $n = 50$ ; when  $n = 300$ ,  $\sigma_e^2$  has the best coverage for mesh 13, while for the others parameters, meshes with higher values of  $c$  have better results.

Table 3 presents the absolute bias of the estimated parameters, for all meshes with  $b = 0.3$ . We observe again that the impact of the `cutoff` parameter is largest, compared to the impact of the `max.edge` parameter. The bias of the estimated parameters is highest when the minimal allowed distance between points is very small. Note that when  $c$  is very small, the mesh can have a highly clustered pattern, whereas when  $c$  is very large, the mesh has only a very limited number of knots. Decreasing the number of knots by increasing the maximal allowed edge in the inner domain, slightly decreases the bias when  $c$  is small. We can observe that for  $\beta_0$  and  $\beta_1$ , the values of bias is really small, and quite often zero, for  $\sigma_e^2$ , mesh 20 has the minimal absolute bias. For the parameter  $\sigma_s^2$ , mesh 21 performs well, for  $k$  meshes with  $c = 0.07$  have the small bias and for  $\phi^*$ , the minimum value of bias is obtained by  $c = 0.01$ . Looking all the parameters together, we can conclude that meshes with  $c = 0.03$  would yield optimal results in this simulation setting. The bias for  $n = 50$  and  $n = 300$  are in Table S.3 and Table S.4, respectively, in Supplementary Material.

The mean square error (MSE) was calculated for each parameter and results are presented in Table S.5 in the Supplementary Material. As we can notice, the value of MSE is high for  $k$  in all meshes, especially for meshes with small values of  $c$  and  $a$ . For  $\beta_0$  almost all meshes have the same results and for  $\beta_1$  meshes with  $c = 0.07$  and  $c = 0.10$  the results are the same and with the minimum value. For  $\sigma_e^2$  the best results for MSE occur for  $c = 0.03$  and for  $\sigma_s^2$  and  $k$  small values for MSE occur for mesh 21, and for  $\phi^*$  meshes 4 and 5 have the minimum value for MSE. Similar results are observed when  $n = 50$  and  $n = 300$  (see Tables S.6 and S.7, respectively, in the Supplementary Material ).

Finally, we also investigated the impact of the mesh on the predictive performance of the model. For each mesh, the coverage and the mean square error (MSE) of the predictions in the sampled locations are calculated. Results are presented in Table 4 (as well as Table S.8 and Table S.9 in the Supplementary Material). Within the groups of meshes with the same value of  $c$ , changing the value of  $a$  has little impact on the MSE and coverage of the predictions. While meshes with the smallest  $c$  value perform the worst in term of coverage, meshes with  $c = 0.03$  have the best coverage and MSE. The results for  $b = 0.4$  and  $b = 0.2$  are similar. In Table 4 we can notice that mesh 20 is one of the meshes with better results and was the mesh that in Table 2 has the best results.



Table 3: Absolute bias of the parameters  $\beta_0$ ,  $\beta_1$ ,  $\sigma_e^2$ ,  $\sigma_s^2$ ,  $k$  and  $\phi^*$  for different meshes with  $b = 0.3$ .

Mesh	Bias for:								Mesh	Bias for:							
	c	a	$\beta_0$	$\beta_1$	$\sigma_e^2$	$\sigma_s^2$	k	$\phi^*$		c	a	$\beta_0$	$\beta_1$	$\sigma_e^2$	$\sigma_s^2$	k	$\phi^*$
1	0.001	0.05	0.00	0.03	0.26	0.27	13.92	0.08	25	0.05	0.05	0.01	0.02	0.06	0.02	0.20	0.10
2		0.09	0.01	0.02	0.28	0.45	13.06	0.09	26		0.09	0.01	0.02	0.07	0.01	0.54	0.09
3		0.13	0.00	0.03	0.28	0.56	11.06	0.08	27		0.13	0.01	0.02	0.10	0.03	0.62	0.11
4		0.17	0.00	0.03	0.28	0.62	9.76	0.08	28		0.17	0.01	0.02	0.12	0.01	0.27	0.11
5		0.19	0.00	0.03	0.28	0.63	9.22	0.08	29		0.19	0.01	0.02	0.13	0.02	0.20	0.11
6		0.20	0.00	0.03	0.28	0.63	8.97	0.07	30		0.20	0.01	0.02	0.13	0.01	0.01	0.10
7	0.005	0.05	0.00	0.03	0.25	0.26	13.14	0.07	31	0.07	0.05	0.01	0.02	0.15	0.01	0.51	0.13
8		0.09	0.00	0.04	0.26	0.42	12.06	0.08	32		0.09	0.01	0.02	0.15	0.01	0.64	0.13
9		0.13	0.00	0.04	0.26	0.52	10.07	0.07	33		0.13	0.01	0.02	0.15	0.01	0.73	0.14
10		0.17	0.00	0.04	0.26	0.58	8.80	0.06	34		0.17	0.01	0.02	0.17	0.01	0.50	0.15
11		0.19	0.00	0.04	0.26	0.59	8.49	0.06	35		0.19	0.01	0.02	0.18	0.05	0.03	0.14
12		0.20	0.00	0.04	0.26	0.59	8.27	0.06	36		0.20	0.01	0.02	0.18	0.06	0.24	0.13
13	0.01	0.05	0.01	0.02	0.20	0.19	9.18	0.03	37	0.10	0.05	0.01	0.02	0.23	0.28	1.73	0.13
14		0.09	0.01	0.02	0.18	0.28	7.79	0.02	38		0.09	0.01	0.02	0.23	0.31	1.78	0.13
15		0.13	0.00	0.03	0.19	0.37	6.79	0.02	39		0.13	0.01	0.02	0.23	0.33	1.75	0.13
16		0.17	0.00	0.03	0.18	0.42	6.03	0.02	40		0.17	0.01	0.02	0.23	0.32	1.68	0.13
17		0.19	0.00	0.03	0.18	0.43	5.74	0.02	41		0.19	0.01	0.02	0.23	0.32	1.65	0.13
18		0.20	0.00	0.03	0.18	0.43	5.57	0.02	42		0.20	0.00	0.03	0.24	0.29	1.33	0.13
19	0.03	0.05	0.01	0.02	0.05	0.02	1.94	0.05	43	0.13	0.05	0.00	0.03	0.29	0.50	2.77	0.12
20		0.09	0.01	0.02	0.01	0.01	0.30	0.08	44		0.09	0.00	0.03	0.29	0.53	2.75	0.12
21		0.13	0.01	0.02	0.03	0.00	0.18	0.09	45		0.13	0.00	0.03	0.30	0.43	2.16	0.12
22		0.17	0.01	0.02	0.04	0.03	0.06	0.09	46		0.17	0.00	0.03	0.30	0.44	2.20	0.12
23		0.19	0.01	0.02	0.04	0.04	0.10	0.09	47		0.19	0.00	0.03	0.30	0.45	2.22	0.12
24		0.20	0.01	0.02	0.04	0.04	0.10	0.08	48		0.20	0.00	0.03	0.30	0.44	2.24	0.12

Table 4: Nominal coverage, in %, and MSE for the variable  $Y$  calculated for each mesh with  $b = 0.3$ , considering 200 simulations.

Mesh	c	a	Coverage(%)	MSE	Mesh	c	a	Coverage(%)	MSE
1	0.001	0.05	18.75	0.28	25	0.05	0.05	90.97	0.21
2		0.09	13.11	0.29	26		0.09	90.79	0.21
3		0.13	11.41	0.29	27		0.13	89.83	0.22
4		0.17	12.24	0.29	28		0.17	89.04	0.22
5		0.19	12.51	0.29	29		0.19	88.89	0.22
6		0.20	12.82	0.29	30		0.20	88.72	0.22
7	0.005	0.05	26.48	0.28	31	0.07	0.05	87.76	0.23
8		0.09	23.54	0.28	32		0.09	87.59	0.23
9		0.13	23.25	0.28	33		0.13	87.61	0.23
10		0.17	23.79	0.28	34		0.17	85.91	0.25
11		0.19	23.82	0.28	35		0.19	85.42	0.25
12		0.20	23.98	0.28	36		0.20	84.98	0.25
13	0.01	0.05	45.17	0.25	37	0.10	0.05	82.06	0.28
14		0.09	48.95	0.25	38		0.09	81.81	0.28
15		0.13	48.67	0.25	39		0.13	81.33	0.28
16		0.17	49.01	0.25	40		0.17	81.28	0.28
17		0.19	48.74	0.25	41		0.19	81.33	0.28
18		0.20	48.85	0.25	42		0.20	81.06	0.28
19	0.03	0.05	85.56	0.21	43	0.13	0.05	75.89	0.32
20		0.09	90.49	0.20	44		0.09	75.53	0.32
21		0.13	90.83	0.20	45		0.13	75.28	0.32
22		0.17	90.84	0.20	46		0.17	75.28	0.32
23		0.19	90.95	0.20	47		0.19	75.33	0.32
24		0.20	90.92	0.21	48		0.20	75.36	0.32

The predictive performance of the model was also investigated for locations not used in the analysis. For  $n = 100$  the predictions was made in 25 locations, and for  $n = 50$  and  $n = 300$  in 13 and 75 locations, respectively. This locations was generated with the simulation study but were withdrawn for control. Table 5 presents the results and we can notice that as the value of  $c$  increases, the coverage is smaller and the MSE has a slight decrease and gets bigger again with  $c = 0.10$ . Within the groups, meshes with  $a = 0.05$  have the best results. For  $n = 50$  and  $n = 300$  the same results are presented in Table S.10 and Table S.11 in the Supplementary Material.

Boxplots of bias for each mesh, considering the 25 extra locations are presented in Figure 2

Table 5: Nominal coverage, in %, and MSE for the response variable calculated for each mesh with  $b = 0.3$ , considering 200 simulations, for 25 locations not in the analysis.

Mesh	c	a	Coverage(%)	MSE	Mesh	c	a	Coverage(%)	MSE
1	0.001	0.05	90.80	0.45	25	0.05	0.05	82.60	0.44
2		0.09	80.26	0.45	26		0.09	82.54	0.44
3		0.13	71.40	0.46	27		0.13	78.60	0.44
4		0.17	62.86	0.47	28		0.17	74.56	0.44
5		0.19	61.14	0.47	29		0.19	73.02	0.45
6		0.20	59.64	0.47	30		0.20	71.58	0.45
7	0.005	0.05	90.76	0.45	31	0.07	0.05	77.78	0.45
8		0.09	80.62	0.45	32		0.09	77.62	0.45
9		0.13	72.50	0.46	33		0.13	77.62	0.45
10		0.17	64.68	0.47	34		0.17	73.82	0.45
11		0.19	63.04	0.47	35		0.19	71.82	0.45
12		0.20	61.50	0.47	36		0.20	70.46	0.46
13	0.01	0.05	89.94	0.44	37	0.10	0.05	71.32	0.46
14		0.09	81.30	0.45	38		0.09	71.06	0.47
15		0.13	73.94	0.45	39		0.13	70.62	0.47
16		0.17	67.38	0.46	40		0.17	70.22	0.47
17		0.19	65.92	0.46	41		0.19	70.12	0.47
18		0.20	65.26	0.46	42		0.20	69.72	0.47
19	0.03	0.05	87.98	0.44	43	0.13	0.05	65.98	0.49
20		0.09	83.10	0.44	44		0.09	65.98	0.49
21		0.13	78.66	0.45	45		0.13	65.94	0.49
22		0.17	74.88	0.45	46		0.17	65.66	0.49
23		0.19	73.60	0.45	47		0.19	65.72	0.49
24		0.20	72.68	0.45	48		0.20	65.96	0.49

(as well as in Figure S.4 and Figure S.5 in the Supplementary Material) and we can notice that there is no difference within and between the groups.

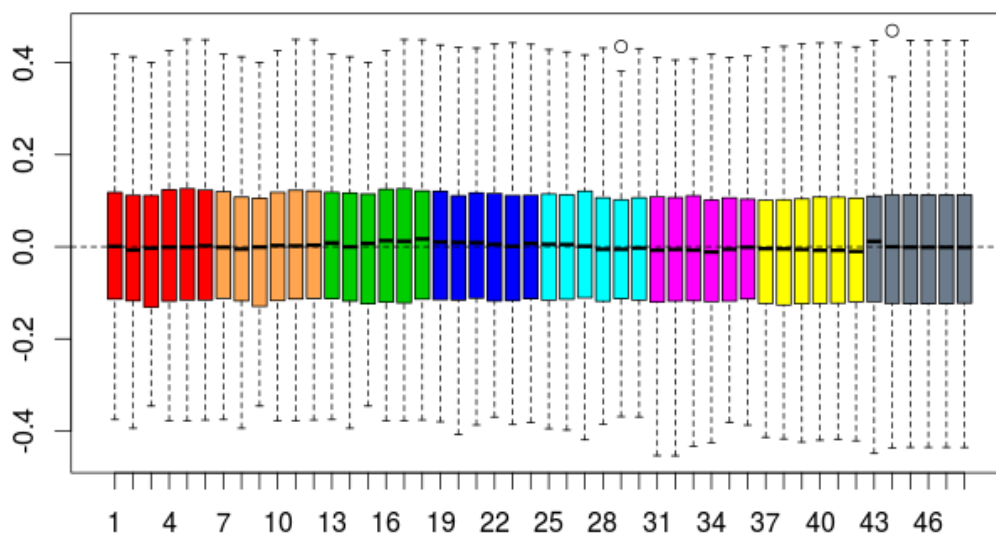


Figure 2: Bias for  $Y$  in 25 extra locations, for all 200 simulations, for  $b = 0.3$ .

### 3.3 Selecting the best mesh

Results in the previous section showed that there is a large impact of the mesh on the inference (parameter estimation and prediction). Also, it was observed that there is not a single mesh which is optimal. Therefore, in this section, we investigate whether we can use the predictive information criteria as described in Section 2.1, to select an optimal mesh.

To perform mesh selection, we calculate DIC, WAIC and logCPO, for each simulation run. To simplify the comparison, we fix  $b = 0.3$  and  $a$  and compare meshes for different values of  $c$ . Figure 3 shows the number of simulations in which the mesh with a particular value of  $c$  was chosen as the best according to DIC (panel I), WAIC (panel II) or logCPO (panel III). In settings where two meshes perform equally good, the lowest value was considered for the two meshes. Looking at Figure 3, we observe an apparent difference between the DIC and WAIC measured on the one hand, and the logCPO on the other hand. Results based on DIC and WAIC are very similar, with smaller values of  $c$  to be preferred in most simulation runs (no matter which  $a$  is selected). LogCPO, on the other hand, seem to select meshes with a larger value of  $c$ , and meshes with  $c = 0.03$  (blue color) seems to stand out.

The mean of DIC, WAIC and logCPO are reported in Table 6 for  $b = 0.3$ . We can observe that meshes with smaller value of  $c$  are selected using DIC and WAIC. For the mean of logCPO, there are multiple meshes with good results and a way to choose one can be the minimum number of knots, which occurs with higher values of  $c$  and  $a$ . If we consider all these three results together, we can choose mesh 20 as the best one, which is the same conclusion as in section 3.2. As we have seen before that the meshes with smaller value of  $c$  lead to larger MSE and bias for inference of covariance parameters, it can be argued that those selection methods are not well suited if interest is only in the covariance function.

Table 6: Mean values of DIC, WAIC and logCPO for meshes with  $b = 0.3$ .

Mesh	c	a	DIC	WAIC	logCPO	Mesh	c	a	DIC	WAIC	logCPO
1	0.001	0.05	-442.09	-448.64	2.07	25	0.05	0.05	230.73	231.21	1.28
2		0.09	-490.14	-500.73	2.09	26		0.09	231.33	231.77	1.28
3		0.13	-504.62	-515.26	2.13	27		0.13	237.21	237.70	1.28
4		0.17	-495.78	-506.18	2.12	28		0.17	240.72	241.35	1.28
5		0.19	-496.70	-506.81	2.11	29		0.19	241.05	241.69	1.28
6		0.20	-492.78	-503.08	2.11	30		0.20	241.55	242.19	1.28
7	0.005	0.05	-369.05	-370.31	1.98	31	0.07	0.05	242.94	243.85	1.28
8		0.09	-389.08	-395.66	1.96	32		0.09	243.20	244.13	1.28
9		0.13	-387.74	-395.32	1.97	33		0.13	243.30	244.24	1.28
10		0.17	-384.21	-389.65	1.96	34		0.17	246.10	247.05	1.28
11		0.19	-383.24	-389.03	1.95	35		0.19	246.78	247.72	1.29
12		0.20	-381.55	-387.75	1.95	36		0.20	247.02	247.92	1.28
13	0.01	0.05	-211.80	-205.13	1.78	37	0.10	0.05	251.05	252.20	1.29
14		0.09	-162.39	-163.09	1.69	38		0.09	250.94	252.10	1.29
15		0.13	-161.75	-166.19	1.70	39		0.13	251.48	252.61	1.29
16		0.17	-156.79	-160.54	1.68	40		0.17	251.50	252.63	1.29
17		0.19	-162.57	-163.38	1.68	41		0.19	251.39	252.54	1.29
18		0.20	-162.23	-162.97	1.68	42		0.20	251.62	252.79	1.29
19	0.03	0.05	155.35	161.35	1.34	43	0.13	0.05	255.85	257.13	1.30
20		0.09	213.02	213.13	1.28	44		0.09	256.22	257.47	1.30
21		0.13	221.37	221.18	1.28	45		0.13	256.55	257.78	1.30
22		0.17	223.23	223.12	1.28	46		0.17	256.55	257.78	1.30
23		0.19	223.54	223.35	1.28	47		0.19	256.49	257.73	1.30
24		0.20	223.71	223.56	1.28	48		0.20	256.57	257.80	1.30

We now evaluate the logCPO, DIC and WAIC criteria for mesh selection over all values of  $a$ ,  $b$  and  $c$ . Figure 4 shows boxplots of parameter estimates based on the mesh with lowest DIC, WAIC or logCPO, obtained in each simulation. For comparison, we also present in this figure the boxplots of the estimates obtained for each parameter with mesh 20, the mesh chosen as

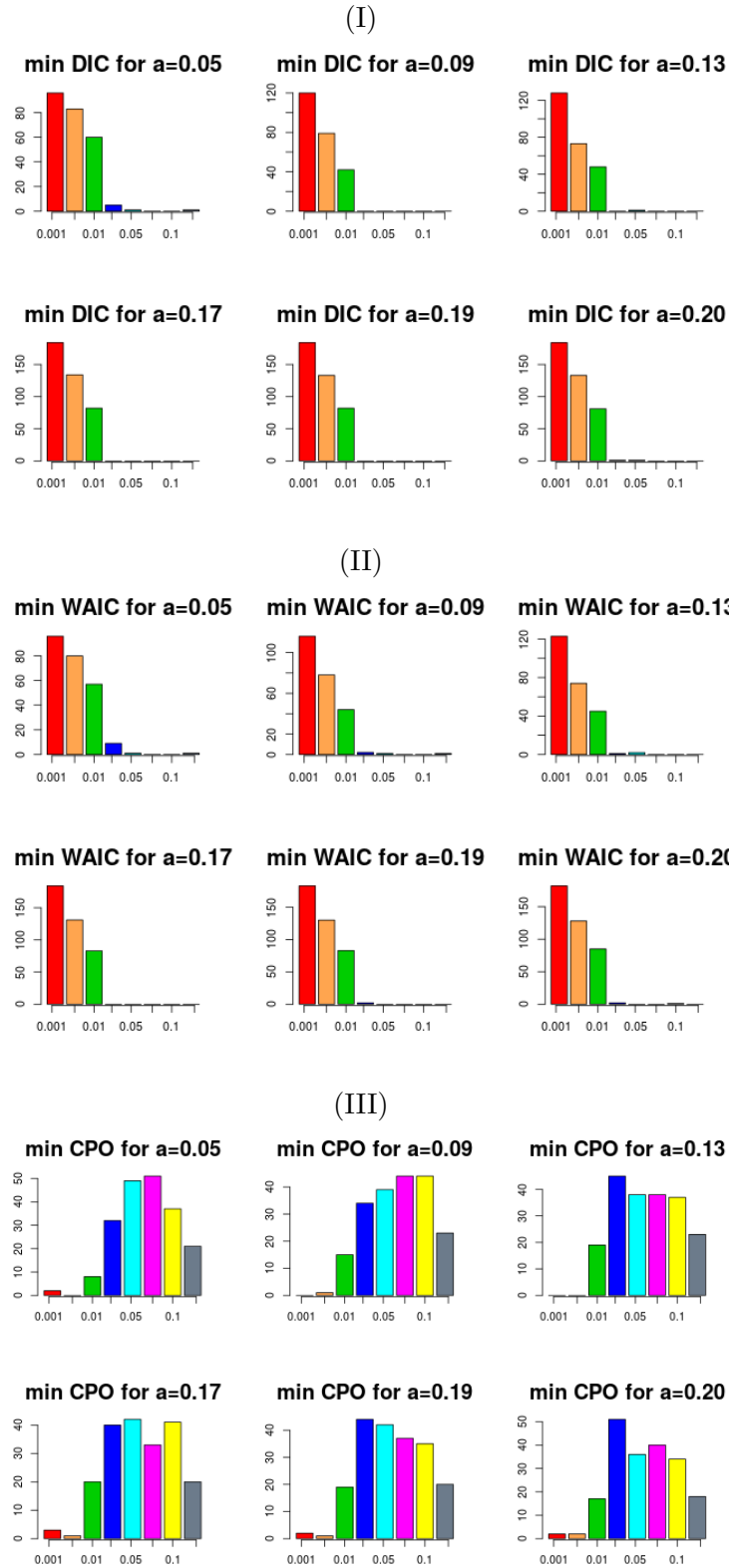


Figure 3: For each value of  $a$ , minimum value of: (I) DIC; (II) WAIC and (III) logCPO, for all 200 simulations, for  $b = 0.3$ .

the one with best overall performance for the chosen simulation settings (based on bias, MSE, coverage of parameter estimates and predictions).

We can observe that the boxplots obtained with mesh 20 are similar to the boxplots obtained

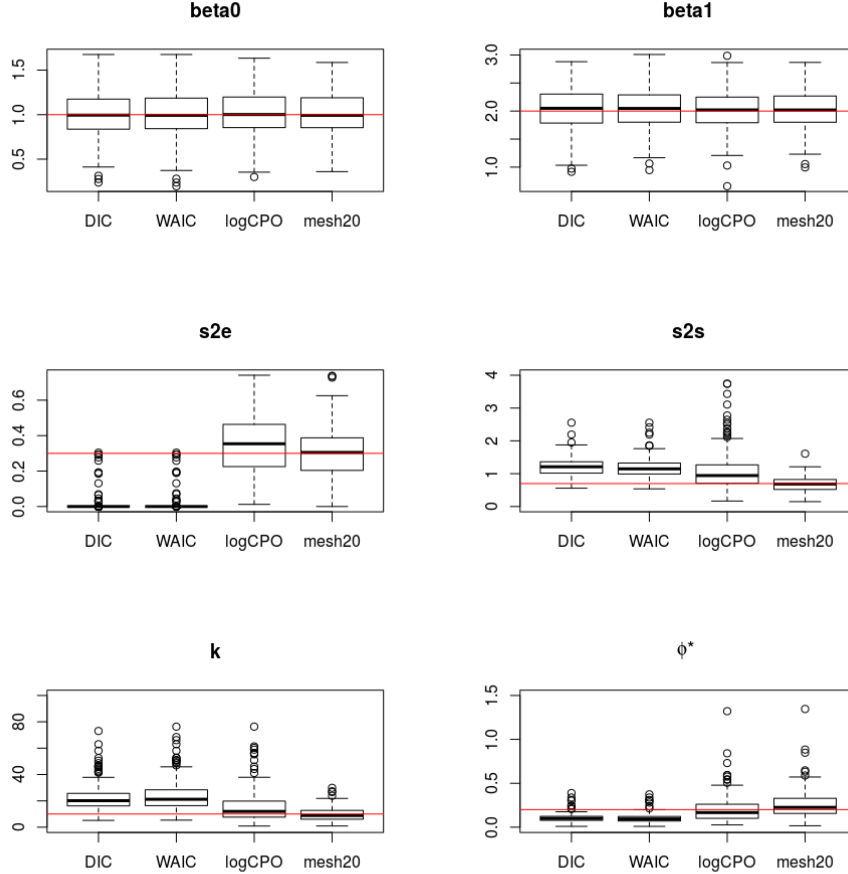


Figure 4: Estimated  $\beta_0$ ,  $\beta_1$ ,  $\sigma_e^2$ ,  $\sigma_s^2$ ,  $k$  and  $\phi^*$ , considering the meshes with minimal DIC, WAIC and logCPO, and based on mesh 20.

for the results of logCPO. Selection of the mesh using DIC and WAIC has bad performance, seen in the large bias of all covariance parameters. Indeed, DIC and WAIC tends to select the mesh with smaller `cutoff` values, and thus the more dense meshes, though it was observed in the previous section that a mesh with smallest  $c$  value leads to larger bias and worse coverage for estimation of the covariance parameters. The logCPO tends to select the mesh with larger `cutoff` values, and thus the more sparse/regular meshes. While the difference between the DIC, WAIC and logCPO would be expected to behave similarly (as they are asymptotically the same), it is important to realize that all methods are only approximations of the predictive accuracy. While DIC and WAIC give reasonable answers in many cases, they only attempt to capture the predictive behavior within the sample, whereas the logCPO captures also out-of-sample prediction error.

Similar results are observed for other sample sizes (see Figures S.6 and S.7 of Supplementary Material). For  $n = 50$  and  $n = 300$ , the best values of DIC and WAIC also occurs for smaller values of  $c$ , as we can see in Table S.12 and Table S.13 of the Supplementary Material, respectively. For logCPO with  $n = 50$ , the best results occur for larger value of  $c$ , especially for  $c = 0.10$ . In the case of  $n = 300$ , meshes with smaller values of  $c$ , mainly  $c = 0.01$ , have the best values of logCPO. Considering the analysis, we can assume that mesh 29 is a good one for  $n = 50$  and mesh 13 for  $n = 300$ . These meshes have plausible and satisfactory results. Figure S.8 and Figure S.9 of the Supplementary Material are figures similar to Figure 4 above and in all this three figures, the boxplot of the chosen mesh is more alike with the boxplot of logCPO, so as told before, logCPO is the best criteria for mesh selection.

Based on these simulation results, it is confirmed that the logCPO criterion is better suited for mesh selection.

## 4 Data Analysis

The data analyzed was the so called Paraná dataset, which is freely available in the geoR package ([Ribeiro;Diggle(2001)]) in R. The data considers average precipitation levels throughout Paraná state, Brazil. Data is available on 143 locations and the response variable represents average winter (dry season) rainfall.

To perform the analysis we take out the linear trend from the variable, because we noticed that this trend lead with non convergence results. To model these data, we assume the model  $y = \beta_0 + \mathbf{s} + \epsilon$ , where  $\mathbf{s}$  is a Matérn spatial random field with  $\alpha = 1.5$ . Considering the range as 380, assumed by a semivariogram analysis, we create eighteen meshes to analyze this data set, namely  $a = c(20, 35, 55, 100, 240, 380)$ ,  $b = 570$  and  $c = c(13, 35, 51)$ . The generated meshes are showed in Figures S.10, S.11 and S.12 of Supplementary Material. All these values were chosen considering the simulation study and for the value of  $a$  was taking into account the value of range, allowing for small values until we reach the expected value of the range, for the value of  $b$  was chosen a value larger than  $a$  and for  $c$  values were considered random in the case that all the coordinates are the inner mesh. In Table 7 we present the number of knots for each of these meshes. We can observe that the number of knots almost does not change for values of  $a$  larger than 100.

Table 7: Number of knots and values for DIC, WAIC and logCPO for each mesh for Paraná data.

Mesh	$c$	$a$	Number knots	DIC	WAIC	logCPO
1	13	20	1235	1305.94	1306.35	4.58
2		35	678	1307.34	1307.46	4.58
3		55	362	1306.53	1306.47	4.58
4		100	234	1307.85	1307.78	4.58
5		240	230	1307.97	1307.91	4.58
6		380	230	1307.97	1307.91	4.58
7	35	20	197	1307.69	1306.64	4.58
8		35	195	1308.14	1307.04	4.58
9		55	194	1307.90	1306.81	4.58
10		100	134	1309.51	1308.59	4.58
11		240	122	1309.71	1308.65	4.58
12		380	122	1309.71	1308.65	4.58
13	51	20	100	1308.18	1307.65	4.58
14		35	100	1308.44	1307.93	4.58
15		55	97	1307.65	1307.09	4.58
16		100	94	1307.60	1307.08	4.58
17		240	77	1307.83	1307.05	4.57
18		380	77	1307.83	1307.05	4.57

The posterior distributions for  $\beta_0$ ,  $\sigma_s^2$ ,  $k$  and  $\phi^*$  are not very different across the considered meshes, as we can observe in Figures S.13, S.14 and S.15 of the Supplementary Material. Table 8 shows the posterior mean estimates for the parameters and we can observe that the choice of the mesh does not have a large impact on the estimates, though mesh 16 was the one that estimates the value for  $\phi^*$  closer to the one that we obtained from the exploratory analysis and also has good results for  $\sigma_s^2$ . The values of DIC, WAIC and logCPO was computed and added into Table 7. As for the posterior estimates, these three criteria also only show minor difference

between the meshes. The smallest results for these three criteria occurs for meshes 1, 17 and 18, in which meshes 17 and 18 are exactly the same. Comparing the results of this meshes with mesh 16 we can say that mesh 16 is better although it has more knots than meshes 17 and 18. So we selected mesh 16 and computed the prediction mean and prediction standard deviation over the study area. This is given in Figure 5.

Table 8: Estimates of the parameters for each mesh.

Mesh	c	a	$\beta_0$	$\sigma_s^2$	$k$	$\phi^*$
1	13	20	-3.04	1004.25	$4 \times 10^{-3}$	530.36
2		35	-2.90	1019.22	$3 \times 10^{-3}$	568.74
3		55	-2.88	1026.20	$3 \times 10^{-3}$	573.44
4		100	-2.87	1020.58	$3 \times 10^{-3}$	588.12
5		240	-2.85	1007.17	$3 \times 10^{-3}$	582.86
6		380	-2.85	1007.17	$3 \times 10^{-3}$	582.86
7	35	20	-2.80	1002.03	$3 \times 10^{-3}$	555.72
8		35	-2.75	1003.72	$3 \times 10^{-3}$	570.49
9		55	-2.77	987.82	$3 \times 10^{-3}$	556.80
10		100	-2.60	1018.22	$3 \times 10^{-3}$	588.27
11		240	-2.37	1063.74	$3 \times 10^{-3}$	618.14
12		380	-2.37	1063.74	$3 \times 10^{-3}$	618.14
13	51	20	-3.25	994.48	$4 \times 10^{-3}$	520.95
14		35	-3.14	979.35	$4 \times 10^{-3}$	512.67
15		55	-3.24	979.76	$4 \times 10^{-3}$	504.03
16		100	-3.14	979.48	$4 \times 10^{-3}$	494.87
17		240	-2.11	1263.75	$3 \times 10^{-3}$	666.64
18		380	-2.11	1263.75	$3 \times 10^{-3}$	666.64

The prediction results is satisfactory since it corroborates with other analyzes with this data.

## 5 Conclusion

The first step to use the SPDE/GMRF approach in INLA with geostatistical data is to create a triangulated mesh over the study area. One way to create the mesh is by telling the locations of the coordinates to serve as a starting point for creating the knots of the mesh. Using a simulation study, we have shown that inferential results depend on the considered mesh. The simulation results indicated that the value of the maximal edge length in the outer domain ( $b$ ), has almost no impact on the results. On the other hand, the choice of the value of the shortest allowed distance between points ( $c$ ), has the largest impact. Thirdly, conditional on a value of  $c$ , the value of the maximal edge length in the inner domain ( $a$ ), also leads to some differences.

Pre-specification of the triangulated mesh is not easy, since it is possible to create a mesh with very good predictive behavior, but that leads to poor covariance parameter estimates. We have used three predictive information criteria, namely DIC, WAIC and CPO, to investigate whether these criteria can be used to select an optimal mesh for a specific data problem. We noticed that the predictive information criteria DIC and WAIC lead to choosing meshes that did not have good results in prediction and estimates. These meshes indeed perform well in terms of coverage and mean squared error for predictions, but do not perform well in the other parts of the analysis, namely the estimation of the covariance parameters. Further, we have noticed that mesh selection using the logCPO leads to better performing meshes overall.

Working with INLA is fast, but selection of the mesh is hindered by the computationally intensive logCPO measurement. While a fast approximating method for CPO calculating is available in INLA, it is very important to ensure that no numerical problems occur. We have

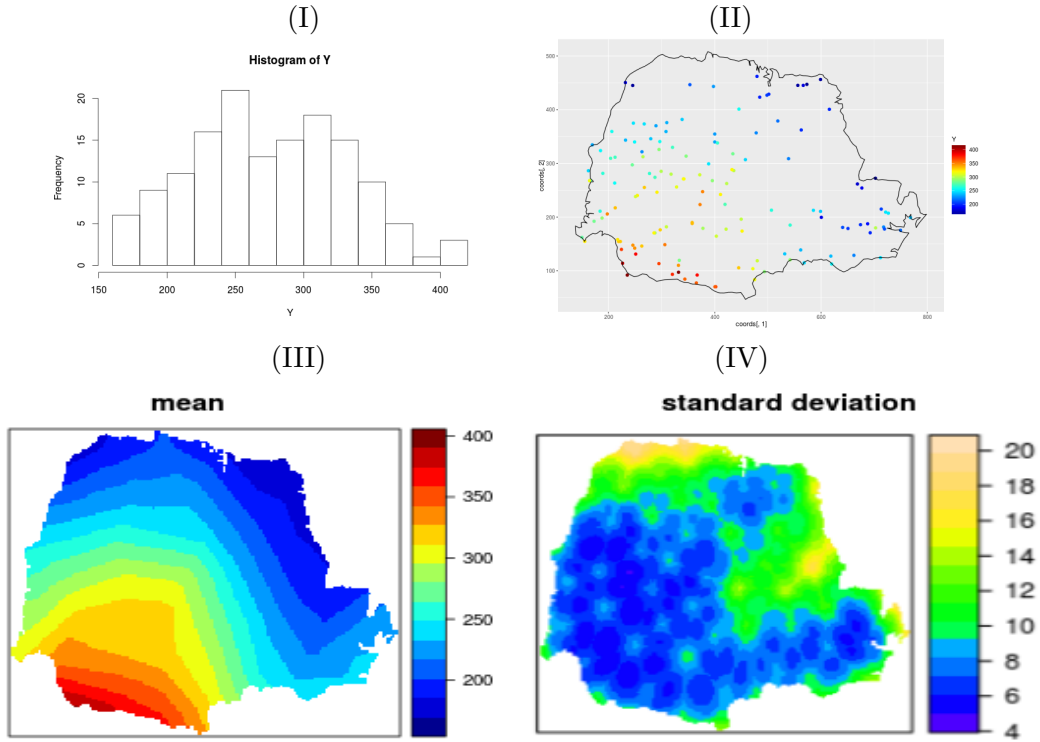


Figure 5: (I) Histogram, (II) plot of data and corresponding values, (III) predicted surface and (IV) prediction standard deviation considering mesh 16.

observed that in many cases, especially with dense meshes, this approximating method does not work and, therefore, CPO needed to be recalculated by refitting the model, leaving out every observation one at a time.

In this paper, we focused on a simple simulation scenario to investigate the impact of different meshes on prediction and estimation of covariance parameters. Further investigation is still needed towards the mesh triangulation using the SPDE/GMRf approach in INLA. For example, in our simulation study the meshes were created considering the coordinates but it is not required that the observed locations are included as nodes in the mesh. Thus, it is also possible to create meshes without the observed coordinates or by using a specific subset of the observed locations. Additionally, situation in which the observed data locations are more clustered or more regular should be investigated in more details.

## 6 Supplementary Material

This file contains additional results of the simulation study in Section 3. (.pdf file)

## Acknowledgements

The first author acknowledge the financial support of the “Ciência sem Fronteiras” program of CNPq (Brazil) under the process number 200573/2015-2. Support from the IAP Research Network P7/06 of the Belgian State (Belgian Science Policy) is also gratefully acknowledged by the second and third author.



## References

- [Bolin;Lindgren (2013)] BOLIN, D.; LINDGREN, F. A comparison between Markov approximations and other methods for large spatial data sets. *Computational Statistics & Data Analysis*, v. 61, p. 7-21, 2013.
- [Bolin;Lindstrom(2014)] BOLIN, D.; LINDSTRÖM, J. Spatial Statistics using R-INLA and Gaussian Markov random fields. *Pan-American Advanced Study Institute*, 15:29:57Z, rev.3691, 2014.
- [Cameletti et al. (2012)] CAMELETTI, M.; LINDGREN, F.; SIMPSON, D., RUE, H. Spatio-temporal modeling of particulate matter concentration through the SPDE approach. *Advances in Statistical Analysis*, v. 97, p. 109-131, 2012.
- [Geisser;Eddy (1979)] GEISSER, S.; EDDY, W. A predictive approach to model selection. *Journal of the American Statistical Association*, Boston, v.74, n.365, p.153-160, 1979.
- [Gelfand et al.(2010)] GELFAND, A. E.; DIGGLE, P. J., FUENTES, M.; GUTTORP, P. (Eds) *Handbook of spatial statistics*. CRC press, 2010.
- [Gelman;Hwang;Vehtari (2014)] GELMAN, A.; HWANG,J.; VEHTARI, A. Understanding predictive information criteria for Bayesian models. *Statistics and Computing*, v. 24, n. 6, p. 997-1016, 2014.
- [Held;Schrodle;Rue(2010)] HELD, L., SCHRODLE, B., RUE, H. Posterior and Cross-validators Predictive Checks: A comparison of MCMC and INLA. In T. Kneib and G. Tutz, editors, *Statistical Modelling and Regression Structures*, p. 91 , 2010.
- [Karagiannis et al. (2013)] KARAGIANNIS-VOULES, D-A, SCHOLTE, R. G. C., GUIMARÉES, L. H., UTZINGER, J., VOUNATSOU, P. Bayesian Geostatistical Modeling of Leishmaniasis Incidence in Brazil. *PLoS Neglected Tropical Diseases*, v. 7, n. 5, e2213. doi:10.1371/journal.pntd.0002213. 2013.
- [Krainski;Rue (2013)] KRAINSKI, E. T.; RUE, H. A short introduction on how to fit a SPDE model with INLA. 2013.
- [Krainski;Lindgren (2014)] KRAINSKI, E. T.; LINDGREN, F. The R-INLA tutorial: SPDE models. 2014.
- [Lindgren (2012)] LINDGREN, F. Continuous domain spatial models in R-INLA. *The ISBA Bulletin*, v. 19, n. 4, 2012.
- [Lindgren;Rue (2015)] LINDGREN, F.; RUE, H. Bayesian spatial modelling with R-INLA. *Journal of Statistical Software*, v. 63, 2015.
- [Lindgren;Rue;Lindstrom (2011)] LINDGREN, F.; RUE, H.; LINDSTRÖM, J. An explicit link between Gaussian fields and Gaussian Markov random fields: The stochastic partial differential equation approach. *Journal of the Royal Statistical Society*, v. 73, p. 423-498, 2011.
- [Ribeiro;Diggle(2001)] RIBEIRO JR., P.J. and DIGGLE, P.J. (2001) geoR: A package for geostatistical analysis. R-NEWS Vol 1, No 2. ISSN 1609-3631. Available for download at: <http://cran.r-project.org/doc/Rnews>.
- [Rue;Martino;Chopin(2009)] RUE, H.; MARTINO, S.; CHOPIN, N. Approximate Bayesian inference for latent Gaussian models by using integrated nested Laplace approximations (with discussion). *Journal of the Royal Statistical Society - Series B*, v.71, Part 2, p.319-392, 2009.

- [Spiegelhalter;Best;Carlin;Linde (2000)] SPIEGELHALTER, D.J.; BEST, N.G.; CARLIN, B.P.; LINDE, A.V.D. Bayesian measures of model complexity and fit. *Journal of the Royal Statistical Society Series B*, London, v.64, n.4, p.583-639, 2000.
- [Vehtari;Gelman (2014)] VEHTARI, A.; GELMAN, A. WAIC and cross-validation in Stan. Submitted. [http://www.stat.columbia.edu/gelman/research/unpublished/waic\\_stan.pdf](http://www.stat.columbia.edu/gelman/research/unpublished/waic_stan.pdf) Accessed, v. 27, n. 2015, p. 5, 2014.
- [Watanabe (2010)] WATANABE, S. Asymptotic equivalence of Bayes cross validation and widely applicable information criterion in singular learning theory. *Journal of Machine Learning Research*, v. 11, p. 3571-3594, 2010.
- [Whittle (1954)] WHITTLE, P. On stationary processes in the plane. ***Biometrika***, v. 41, p. 434-449, 1954.

# On the choice of the mesh for the analysis of geostatistical data using R-INLA - Supplementary Material

**Ana Julia Righetto**

Departamento de Ciências Exatas,  
Universidade de São Paulo,  
13418-900, Piracicaba, SP, Brazil.

e-mail: *ajrighetto@gmail.com*

**Christel Faes and Yannick Vandendijck**

Interuniversity Institute for Biostatistics and  
statistical Bioinformatics (I-BioStat),  
Hasselt University, Hasselt, Belgium

e-mail: *christel.faes@uhasselt.be* and *yannick.vandendijck@uhasselt.be*

**Paulo Justiniano Ribeiro Junior**

Departamento de Estatística,  
Universidade Federal do Paraná, Brazil

e-mail: *paulojus@ufpr.br*

## 1 Additional simulations results

In Section 3 of the paper a simulation study is presented with  $n = 100$ . In this section of the supplementary materials we provide the results of the simulation study considering  $n = 50$  and  $n = 300$ .

The colours of the graphics in the following sessions are: red for  $c=0.001$ , orange for  $c=0.005$ , green for  $c=0.01$ , blue for  $c=0.03$ , light blue for  $c=0.05$ , pink for  $c=0.07$ , yellow for  $c=0.10$  and grey for  $c=0.13$ . And in each group of these colours, the value of  $a$  increases from left to right.

### 1.1 Simulation study with $n=50$ , $n=100$ and $n=300$

#### Impact of mesh on inference

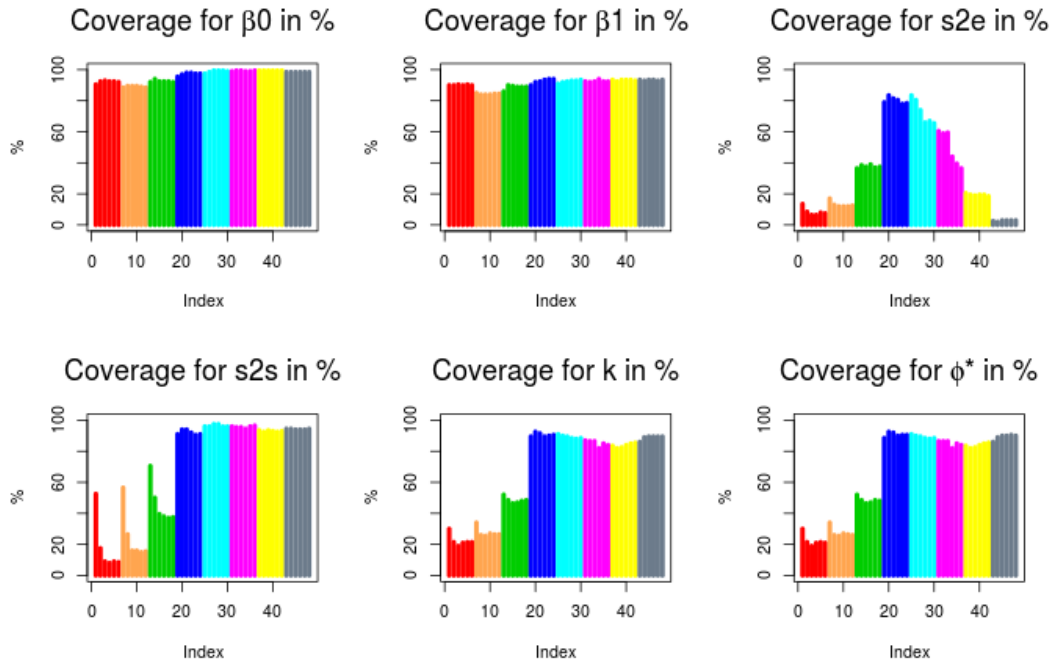


Figure S.1: Coverage of the meshes for:  $\beta_0$ ,  $\beta_1$ ,  $\sigma_e^2$ ,  $\sigma_s^2$ ,  $k$  and  $\phi^*$  with  $n=100$ .

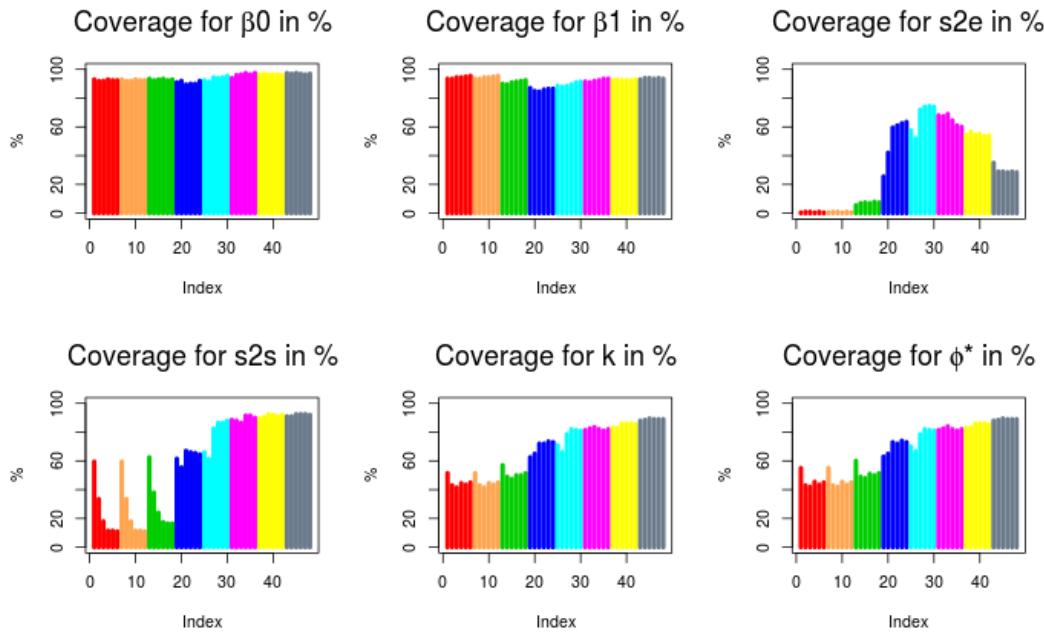


Figure S.2: Coverage of the meshes for:  $\beta_0$ ,  $\beta_1$ ,  $\sigma_e^2$ ,  $\sigma_s^2$ ,  $k$  and  $\phi^*$  with  $n=50$ .

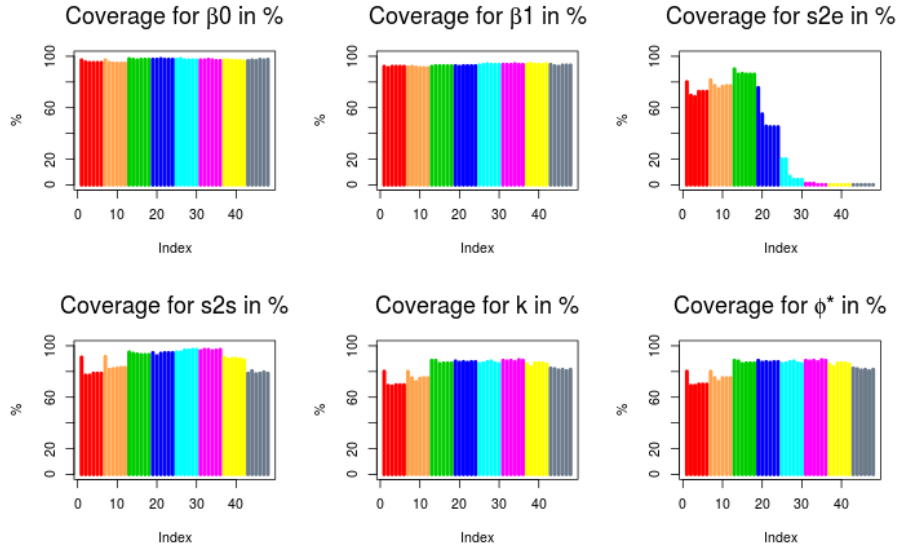


Figure S.3: Coverage of the meshes for:  $\beta_0$ ,  $\beta_1$ ,  $\sigma_e^2$ ,  $\sigma_s^2$ ,  $k$  and  $\phi^*$  with  $n=300$ .

Table S.1: Coverage, in %, of the 95% credible intervals of the parameters  $\beta_0$ ,  $\beta_1$ ,  $\sigma_e^2$ ,  $\sigma_s^2$ ,  $k$  and  $\phi^*$  for different meshes with  $b = 0.3$ , for  $n = 50$ .

Mesh	$c$	$a$	Coverage in % for:						Mesh	$c$	$a$	Coverage in % for:					
			$\beta_0$	$\beta_1$	$\sigma_e^2$	$\sigma_s^2$	$k$	$\phi^*$				$\beta_0$	$\beta_1$	$\sigma_e^2$	$\sigma_s^2$	$k$	$\phi^*$
1	0.001	0.05	93.00	93.50	0.50	59.50	51.50	55.00	25	0.05	0.05	92.50	88.50	57.50	66.00	71.00	70.00
2		0.09	92.00	93.50	1.00	33.50	43.00	43.00	26	0.09	0.09	91.50	88.00	52.00	61.50	66.00	66.50
3		0.13	92.00	94.50	1.00	18.00	41.50	42.00	27	0.13	0.13	94.50	88.50	72.00	82.50	78.50	78.50
4		0.17	93.00	94.50	0.50	11.50	44.50	45.50	28	0.17	0.17	94.00	89.50	74.00	86.50	82.00	82.00
5		0.19	92.50	95.00	1.00	11.50	43.50	43.50	29	0.19	0.19	94.50	91.00	74.50	86.50	81.50	81.50
6		0.20	92.50	95.50	0.50	11.00	45.00	45.00	30	0.20	0.20	95.50	91.50	74.00	88.00	81.00	81.00
7	0.005	0.05	93.00	93.50	0.50	59.50	51.50	55.00	31	0.07	0.05	94.00	91.50	68.00	88.50	81.50	81.50
8		0.09	92.00	93.50	1.00	33.50	43.00	43.00	32	0.09	0.09	96.00	91.00	67.50	88.00	82.50	82.50
9		0.13	92.00	94.50	1.00	18.00	41.50	42.00	33	0.13	0.13	96.50	92.00	69.00	86.50	83.50	84.00
10		0.17	93.00	94.50	0.50	11.50	44.50	45.50	34	0.17	0.17	97.50	92.50	64.50	91.50	82.00	82.00
11		0.19	92.50	95.00	1.00	11.50	43.50	43.50	35	0.19	0.19	96.50	93.50	61.00	91.50	81.00	81.00
12		0.20	92.50	95.50	0.50	11.00	45.00	45.00	36	0.20	0.20	97.50	93.50	60.00	90.00	82.00	82.00
13	0.01	0.05	93.50	90.00	5.50	62.50	57.00	60.00	37	0.10	0.05	96.50	92.50	54.50	89.50	83.00	83.00
14		0.09	92.50	89.50	7.00	38.00	49.00	49.00	38	0.09	0.09	97.00	93.00	56.50	90.50	83.00	83.00
15		0.13	93.00	91.00	7.50	24.00	47.50	48.00	39	0.13	0.13	96.50	92.50	54.50	92.50	86.00	86.00
16		0.17	93.50	91.50	7.00	17.50	50.00	51.00	40	0.17	0.17	96.50	92.50	55.00	92.00	86.00	86.00
17		0.19	92.50	92.00	8.00	16.50	50.00	50.00	41	0.19	0.19	96.50	92.50	53.50	91.00	86.00	86.00
18		0.20	93.00	92.50	7.50	16.50	51.50	51.50	42	0.20	0.20	96.00	93.00	54.00	92.00	85.50	85.50
19	0.03	0.05	91.00	87.00	25.50	61.50	62.50	63.00	43	0.13	0.05	97.50	93.00	35.00	91.00	88.00	88.00
20		0.09	92.00	85.00	42.00	55.50	65.00	65.00	44	0.09	0.09	97.00	94.00	29.00	91.00	88.50	88.50
21		0.13	89.50	84.50	59.50	67.00	72.00	73.00	45	0.13	0.13	97.50	94.00	29.00	92.50	89.50	89.50
22		0.17	90.00	86.00	61.00	66.00	72.00	72.00	46	0.17	0.17	97.00	93.50	28.50	92.50	89.00	89.00
23		0.19	90.00	86.50	62.50	65.50	73.50	74.00	47	0.19	0.19	96.50	94.00	29.00	92.50	89.00	89.00
24		0.20	92.00	86.50	63.50	64.50	73.00	73.00	48	0.20	0.20	97.00	93.50	28.50	92.00	89.00	89.00

Table S.2: Coverage, in %, of the 95% credible intervals of the parameters  $\beta_0$ ,  $\beta_1$ ,  $\sigma_e^2$ ,  $\sigma_s^2$ ,  $k$  and  $\phi^*$  for different meshes with  $b = 0.3$ , for  $n = 300$ .

Mesh	$c$	$a$	Coverage in % for:						Mesh	$c$	$a$	Coverage in % for:					
			$\beta_0$	$\beta_1$	$\sigma_e^2$	$\sigma_s^2$	$k$	$\phi^*$				$\beta_0$	$\beta_1$	$\sigma_e^2$	$\sigma_s^2$	$k$	$\phi^*$
1	0.001	0.05	97.00	92.00	80.00	91.00	80.00	80.00	25	0.05	0.05	97.50	93.00	20.00	95.00	86.00	86.00
2		0.09	95.50	91.00	69.50	77.00	69.00	69.00	26		0.09	98.00	93.50	20.00	95.00	86.50	86.50
3		0.13	95.00	92.00	68.50	77.00	68.50	69.00	27		0.13	97.00	94.00	6.50	96.50	87.50	87.50
4		0.17	95.00	92.00	72.50	78.50	69.50	70.00	28		0.17	97.00	93.50	4.00	96.50	88.00	88.00
5		0.19	95.00	92.00	72.50	78.50	69.50	70.00	29		0.19	97.00	93.50	4.00	97.00	86.50	86.50
6		0.20	95.00	92.00	72.50	78.50	69.50	70.00	30		0.20	97.00	93.50	4.00	97.00	86.00	86.00
7	0.005	0.05	97.00	91.50	81.50	91.50	80.00	80.00	31	0.07	0.05	97.00	93.50	1.00	96.00	88.50	88.50
8		0.09	95.00	92.00	77.00	81.50	75.00	75.00	32		0.09	97.00	93.50	1.00	97.00	88.00	88.00
9		0.13	94.50	91.50	74.50	82.00	72.00	72.00	33		0.13	97.50	93.50	1.00	97.00	88.50	88.50
10		0.17	94.50	91.00	76.50	82.50	74.50	75.00	34		0.17	97.00	94.00	0.00	96.00	87.50	87.50
11		0.19	94.50	91.00	77.00	83.00	75.00	75.00	35		0.19	96.50	93.50	0.00	96.50	89.00	89.00
12		0.20	94.50	91.00	77.00	83.00	75.00	75.00	36		0.20	96.50	93.50	0.00	97.00	88.50	88.50
13	0.01	0.05	98.00	92.00	90.00	95.00	88.50	88.50	37	0.10	0.05	97.00	93.50	0.00	91.00	86.00	85.50
14		0.09	97.50	92.50	86.00	94.00	88.50	88.00	38		0.09	97.00	94.50	0.00	89.50	83.50	83.50
15		0.13	97.00	92.50	86.50	93.50	86.00	86.00	39		0.13	96.50	93.50	0.00	90.00	86.50	86.50
16		0.17	97.50	92.50	86.00	93.00	86.50	86.50	40		0.17	96.50	93.50	0.00	90.00	86.50	86.50
17		0.19	97.50	92.50	86.00	93.00	86.50	86.50	41		0.19	96.50	93.50	0.00	89.50	86.50	86.50
18		0.20	97.50	92.50	86.00	93.00	86.50	86.50	42		0.20	96.00	94.00	0.00	89.00	85.50	85.50
19	0.03	0.05	97.50	92.50	75.50	94.50	88.00	88.50	43	0.13	0.05	96.50	93.50	0.00	78.50	82.50	82.50
20		0.09	97.50	92.00	55.00	92.00	87.00	87.00	44		0.09	97.00	92.50	0.00	80.50	82.00	82.00
21		0.13	98.00	92.50	45.50	94.00	87.50	87.50	45		0.13	96.50	92.00	0.00	78.00	81.00	81.00
22		0.17	97.50	92.50	45.00	94.50	87.00	87.00	46		0.17	97.50	93.00	0.00	78.50	81.50	81.50
23		0.19	97.50	92.50	45.00	94.50	87.50	87.50	47		0.19	97.00	93.00	0.00	79.50	80.50	80.50
24		0.20	97.50	92.50	45.00	94.50	87.50	87.50	48		0.20	97.50	93.00	0.00	78.50	81.50	81.50

Table S.3: Absolute bias of the parameters  $\beta_0$ ,  $\beta_1$ ,  $\sigma_e^2$ ,  $\sigma_s^2$ ,  $k$  and  $\phi^*$  for different meshes with  $b = 0.3$ , for  $n = 50$ .

Mesh	$c$	$a$	Bias for:						Mesh	$c$	$a$	Bias for:					
			$\beta_0$	$\beta_1$	$\sigma_e^2$	$\sigma_s^2$	$k$	$\phi^*$				$\beta_0$	$\beta_1$	$\sigma_e^2$	$\sigma_s^2$	$k$	$\phi^*$
1	0.001	0.05	0.03	0.00	0.30	0.67	18.57	0.08	25	0.05	0.05	0.04	0.02	0.08	0.49	6.61	0.10
2		0.09	0.02	0.00	0.30	0.62	14.04	0.08	26		0.09	0.04	0.02	0.09	0.63	7.91	0.12
3		0.13	0.03	0.00	0.30	0.73	11.33	0.08	27		0.13	0.03	0.01	0.01	0.25	2.76	0.16
4		0.17	0.02	0.00	0.30	0.83	9.35	0.07	28		0.17	0.04	0.02	0.04	0.31	2.16	0.19
5		0.19	0.02	0.00	0.30	0.85	8.53	0.07	29		0.19	0.04	0.03	0.05	0.32	2.00	0.19
6		0.20	0.02	0.00	0.30	0.87	8.35	0.07	30		0.20	0.04	0.03	0.06	0.30	1.72	0.19
7	0.005	0.05	0.03	0.00	0.30	0.67	18.57	0.08	31	0.07	0.05	0.03	0.01	0.08	0.29	1.22	0.22
8		0.09	0.02	0.00	0.30	0.62	14.04	0.08	32		0.09	0.03	0.00	0.09	0.46	1.92	0.22
9		0.13	0.03	0.00	0.30	0.73	11.33	0.08	33		0.13	0.03	0.01	0.09	0.21	0.68	0.23
10		0.17	0.02	0.00	0.30	0.83	9.35	0.07	34		0.17	0.03	0.01	0.13	0.21	0.59	0.24
11		0.19	0.02	0.00	0.30	0.85	8.53	0.07	35		0.19	0.03	0.01	0.15	0.33	1.11	0.25
12		0.20	0.02	0.00	0.30	0.87	8.35	0.07	36		0.20	0.03	0.01	0.16	0.38	1.33	0.25
13	0.01	0.05	0.02	0.00	0.28	0.62	15.71	0.06	37	0.10	0.05	0.03	0.01	0.19	0.36	1.35	0.24
14		0.09	0.02	0.01	0.28	0.56	11.97	0.06	38		0.09	0.03	0.01	0.20	0.48	1.48	0.25
15		0.13	0.02	0.01	0.28	0.66	9.71	0.06	39		0.13	0.03	0.01	0.19	0.25	0.95	0.25
16		0.17	0.02	0.01	0.28	0.75	7.94	0.05	40		0.17	0.03	0.01	0.19	0.22	0.46	0.25
17		0.19	0.02	0.01	0.28	0.77	7.18	0.05	41		0.19	0.03	0.01	0.20	0.22	0.41	0.26
18		0.20	0.02	0.01	0.28	0.79	7.15	0.05	42		0.20	0.03	0.01	0.20	0.29	1.10	0.25
19	0.03	0.05	0.02	0.02	0.21	0.32	9.56	0.00	43	0.13	0.05	0.03	0.01	0.27	0.64	2.64	0.21
20		0.09	0.02	0.01	0.16	0.53	9.04	0.05	44		0.09	0.03	0.01	0.28	0.52	2.37	0.21
21		0.13	0.01	0.03	0.10	0.42	4.57	0.10	45		0.13	0.03	0.01	0.28	0.50	2.08	0.22
22		0.17	0.02	0.03	0.09	0.65	5.25	0.09	46		0.17	0.03	0.01	0.28	0.50	2.07	0.21
23		0.19	0.02	0.02	0.09	0.57	4.54	0.09	47		0.19	0.03	0.01	0.28	0.49	2.21	0.21
24		0.20	0.02	0.02	0.08	0.60	4.39	0.11	48		0.20	0.03	0.01	0.28	0.50	2.06	0.22

Table S.4: Absolute bias of the parameters  $\beta_0$ ,  $\beta_1$ ,  $\sigma_e^2$ ,  $\sigma_s^2$ ,  $k$  and  $\phi^*$  for different meshes with  $b = 0.3$ , for  $n = 300$ .

Mesh	c	a	Bias for:						Mesh	c	a	Bias for:					
			$\beta_0$	$\beta_1$	$\sigma_e^2$	$\sigma_s^2$	k	$\phi^*$				$\beta_0$	$\beta_1$	$\sigma_e^2$	$\sigma_s^2$	k	$\phi^*$
1	0.001	0.05	0.02	0.01	0.03	0.01	1.64	0.01	25	0.05	0.05	0.02	0.01	0.12	0.05	1.71	0.07
2		0.09	0.02	0.01	0.05	0.05	3.24	0.00	26		0.09	0.02	0.01	0.12	0.05	1.69	0.07
3		0.13	0.02	0.01	0.05	0.07	3.12	0.00	27		0.13	0.02	0.01	0.14	0.05	1.46	0.07
4		0.17	0.02	0.01	0.05	0.07	2.91	0.00	28		0.17	0.02	0.01	0.15	0.04	1.38	0.07
5		0.19	0.02	0.01	0.05	0.07	2.89	0.00	29		0.19	0.02	0.01	0.15	0.03	1.35	0.07
6		0.20	0.02	0.01	0.05	0.07	2.89	0.00	30		0.20	0.02	0.01	0.15	0.03	1.36	0.07
7	0.005	0.05	0.02	0.01	0.03	0.01	1.34	0.01	31	0.07	0.05	0.02	0.01	0.17	0.00	0.75	0.06
8		0.09	0.02	0.01	0.03	0.02	2.29	0.01	32		0.09	0.02	0.01	0.17	0.00	0.78	0.06
9		0.13	0.02	0.01	0.04	0.05	2.35	0.00	33		0.13	0.02	0.01	0.17	0.00	0.77	0.06
10		0.17	0.02	0.01	0.03	0.05	2.14	0.00	34		0.17	0.02	0.01	0.20	0.02	0.29	0.05
11		0.19	0.02	0.01	0.03	0.04	2.05	0.00	35		0.19	0.02	0.01	0.20	0.04	0.06	0.05
12		0.20	0.02	0.01	0.03	0.04	2.05	0.00	36		0.20	0.02	0.01	0.20	0.04	0.01	0.05
13	0.01	0.05	0.02	0.01	0.01	0.04	0.36	0.03	37	0.10	0.05	0.02	0.01	0.24	0.25	1.23	0.04
14		0.09	0.02	0.01	0.01	0.03	0.08	0.03	38		0.09	0.02	0.01	0.25	0.24	1.06	0.04
15		0.13	0.02	0.01	0.01	0.02	0.14	0.02	39		0.13	0.02	0.01	0.24	0.24	1.00	0.04
16		0.17	0.02	0.01	0.01	0.01	0.10	0.02	40		0.17	0.02	0.01	0.24	0.24	1.00	0.04
17		0.19	0.02	0.01	0.01	0.01	0.10	0.02	41		0.19	0.02	0.01	0.25	0.25	1.10	0.04
18		0.20	0.02	0.01	0.01	0.01	0.10	0.02	42		0.20	0.02	0.01	0.25	0.26	1.21	0.04
19	0.03	0.05	0.02	0.01	0.06	0.04	1.56	0.06	43	0.13	0.05	0.02	0.01	0.29	0.64	2.85	0.04
20		0.09	0.02	0.01	0.08	0.06	1.81	0.07	44		0.09	0.02	0.01	0.30	0.70	3.14	0.04
21		0.13	0.02	0.01	0.09	0.05	1.62	0.06	45		0.13	0.01	0.01	0.30	$35x10^{100}$	3.00	25.75
22		0.17	0.02	0.01	0.09	0.04	1.61	0.06	46		0.17	0.02	0.01	0.30	$48x10^{100}$	3.11	27107.18
23		0.19	0.02	0.01	0.09	0.04	1.60	0.06	47		0.19	0.02	0.01	0.30	$48x10^{100}$	3.06	27107.18
24		0.20	0.02	0.01	0.09	0.04	1.60	0.06	48		0.20	0.02	0.01	0.30	$48x10^{100}$	3.11	27107.18

Table S.5: MSE of the parameters  $\beta_0$ ,  $\beta_1$ ,  $\sigma_e^2$ ,  $\sigma_s^2$ ,  $k$  and  $\phi^*$  for different meshes with  $b = 0.3$ , with  $n=100$ .

Mesh	c	a	MSE for:						Mesh	c	a	MSE for:					
			$\beta_0$	$\beta_1$	$\sigma_e^2$	$\sigma_s^2$	k	$\phi^*$				$\beta_0$	$\beta_1$	$\sigma_e^2$	$\sigma_s^2$	k	$\phi^*$
1	0.001	0.05	0.07	0.12	0.08	0.29	543.04	0.02	25	0.05	0.05	0.06	0.11	0.02	0.08	88.57	0.07
2		0.09	0.07	0.12	0.08	0.34	299.48	0.02	26		0.09	0.06	0.11	0.02	0.12	131.08	0.06
3		0.13	0.06	0.12	0.08	0.40	182.82	0.02	27		0.13	0.06	0.11	0.02	0.07	36.54	0.07
4		0.17	0.06	0.12	0.08	0.48	144.96	0.01	28		0.17	0.06	0.11	0.03	0.08	51.22	0.08
5		0.19	0.06	0.12	0.08	0.47	127.04	0.01	29		0.19	0.06	0.11	0.03	0.10	59.79	0.07
6		0.20	0.06	0.12	0.08	0.48	122.49	0.02	30		0.20	0.06	0.10	0.03	0.09	46.20	0.06
7	0.005	0.05	0.07	0.14	0.08	0.30	544.10	0.02	31	0.07	0.05	0.06	0.10	0.03	0.09	45.91	0.10
8		0.09	0.07	0.14	0.08	0.33	285.95	0.02	32		0.09	0.06	0.10	0.03	0.10	46.08	0.10
9		0.13	0.07	0.14	0.08	0.38	171.38	0.02	33		0.13	0.06	0.10	0.03	0.09	41.33	0.11
10		0.17	0.07	0.14	0.08	0.44	131.29	0.02	34		0.17	0.06	0.10	0.04	0.14	49.59	0.12
11		0.19	0.07	0.14	0.08	0.46	121.33	0.02	35		0.19	0.06	0.10	0.05	0.22	66.93	0.11
12		0.20	0.07	0.14	0.08	0.45	115.09	0.02	36		0.20	0.06	0.10	0.05	0.23	69.40	0.11
13	0.01	0.05	0.07	0.14	0.06	0.28	424.82	0.04	37	0.10	0.05	0.06	0.10	0.06	1.16	123.40	0.11
14		0.09	0.07	0.14	0.06	0.24	202.96	0.04	38		0.09	0.06	0.10	0.06	1.96	125.43	0.12
15		0.13	0.07	0.13	0.06	0.26	120.75	0.04	39		0.13	0.06	0.10	0.07	2.32	138.98	0.11
16		0.17	0.07	0.13	0.06	0.32	100.72	0.04	40		0.17	0.06	0.10	0.07	1.91	130.67	0.12
17		0.19	0.07	0.13	0.06	0.33	91.92	0.04	41		0.19	0.06	0.10	0.07	1.93	127.96	0.11
18		0.20	0.07	0.13	0.06	0.33	86.29	0.04	42		0.20	0.06	0.11	0.07	2.44	111.41	0.11
19	0.03	0.05	0.06	0.12	0.03	0.07	87.72	0.06	43	0.13	0.05	0.06	0.11	0.09	1.87	130.20	0.12
20		0.09	0.06	0.11	0.02	0.14	88.41	0.06	44		0.09	0.06	0.11	0.10	2.20	133.10	0.12
21		0.13	0.06	0.11	0.02	0.06	31.88	0.07	45		0.13	0.06	0.11	0.10	1.33	107.18	0.11
22		0.17	0.06	0.11	0.02	0.07	34.07	0.07	46		0.17	0.06	0.11	0.10	1.38	108.93	0.11
23		0.19	0.06	0.11	0.02	0.08	32.10	0.07	47		0.19	0.06	0.11	0.10	1.42	112.95	0.11
24		0.20	0.06	0.11	0.02	0.08	32.60	0.06	48		0.20	0.06	0.11	0.10	1.37	109.74	0.12

Table S.6: MSE of the parameters  $\beta_0, \beta_1, \sigma_e^2, \sigma_s^2, k$  and  $\phi^*$  for different meshes with  $b = 0.3$ , for  $n = 50$ .

Mesh	MSE for:								Mesh	MSE for:							
	$c$	$a$	$\beta_0$	$\beta_1$	$\sigma_e^2$	$\sigma_s^2$	$k$	$\phi^*$		$c$	$a$	$\beta_0$	$\beta_1$	$\sigma_e^2$	$\sigma_s^2$	$k$	$\phi^*$
1	0.001	0.05	0.10	0.20	0.09	13.77	2187.42	0.01	25	0.05	0.05	0.11	0.24	0.06	1.69	360.94	0.17
2		0.09	0.10	0.19	0.09	1.18	541.03	0.01	26	0.09	0.11	0.25	0.06	3.23	491.41	0.24	
3		0.13	0.10	0.19	0.09	0.86	266.87	0.01	27	0.13	0.10	0.22	0.04	0.78	204.33	0.21	
4		0.17	0.11	0.19	0.09	1.00	179.91	0.01	28	0.17	0.11	0.22	0.04	1.24	174.91	0.28	
5		0.19	0.11	0.19	0.09	0.95	142.91	0.01	29	0.19	0.11	0.22	0.04	1.38	167.62	0.29	
6		0.20	0.11	0.19	0.09	1.04	140.73	0.01	30	0.20	0.11	0.22	0.04	1.13	156.68	0.30	
7	0.005	0.05	0.10	0.20	0.09	13.77	2187.42	0.01	31	0.07	0.05	0.10	0.21	0.05	2.45	175.99	0.31
8		0.09	0.10	0.19	0.09	1.18	541.03	0.01	32	0.09	0.10	0.21	0.05	6.31	222.77	0.32	
9		0.13	0.10	0.19	0.09	0.86	266.87	0.01	33	0.13	0.10	0.21	0.05	0.92	132.95	0.31	
10		0.17	0.11	0.19	0.09	1.00	179.91	0.01	34	0.17	0.10	0.21	0.05	0.70	119.57	0.32	
11		0.19	0.11	0.19	0.09	0.95	142.91	0.01	35	0.19	0.10	0.20	0.06	2.35	176.24	0.34	
12		0.20	0.11	0.19	0.09	1.04	140.73	0.01	36	0.20	0.10	0.20	0.06	4.00	201.84	0.34	
13	0.01	0.05	0.11	0.23	0.09	13.72	1969.76	0.02	37	0.10	0.05	0.10	0.20	0.07	2.05	140.64	0.33
14		0.09	0.11	0.23	0.09	1.10	452.62	0.02	38	0.09	0.10	0.20	0.07	5.62	145.15	0.36	
15		0.13	0.11	0.24	0.09	0.75	214.01	0.03	39	0.13	0.10	0.20	0.07	0.92	100.31	0.36	
16		0.17	0.11	0.23	0.09	0.89	140.82	0.03	40	0.17	0.10	0.20	0.07	0.81	85.61	0.37	
17		0.19	0.12	0.24	0.08	0.85	111.39	0.03	41	0.19	0.10	0.20	0.07	0.79	86.43	0.38	
18		0.20	0.12	0.23	0.08	0.95	117.64	0.03	42	0.20	0.10	0.20	0.07	1.38	107.11	0.36	
19	0.03	0.05	0.12	0.24	0.07	0.44	406.22	0.09	43	0.13	0.05	0.10	0.20	0.11	5.73	145.46	0.34
20		0.09	0.12	0.24	0.06	2.11	591.50	0.12	44	0.09	0.10	0.20	0.11	3.76	137.79	0.33	
21		0.13	0.12	0.25	0.05	1.14	230.60	0.16	45	0.13	0.10	0.20	0.11	3.83	132.40	0.34	
22		0.17	0.12	0.25	0.05	3.87	283.34	0.16	46	0.17	0.10	0.20	0.11	3.84	130.75	0.34	
23		0.19	0.11	0.24	0.05	1.95	214.86	0.16	47	0.19	0.10	0.20	0.11	2.93	129.65	0.33	
24		0.20	0.11	0.24	0.05	2.08	215.06	0.24	48	0.20	0.10	0.20	0.11	3.83	131.23	0.34	

Table S.7: MSE of the parameters  $\beta_0, \beta_1, \sigma_e^2, \sigma_s^2, k$  and  $\phi^*$  for different meshes with  $b = 0.3$ , for  $n = 300$ .

Mesh	MSE for:								Mesh	MSE for:							
	$c$	$a$	$\beta_0$	$\beta_1$	$\sigma_e^2$	$\sigma_s^2$	$k$	$\phi^*$		$c$	$a$	$\beta_0$	$\beta_1$	$\sigma_e^2$	$\sigma_s^2$	$k$	$\phi^*$
1	0.001	0.05	0.03	0.03	0.01	0.02	50.01	0.01	25	0.05	0.05	0.03	0.03	0.02	0.03	12.56	0.01
2		0.09	0.03	0.03	0.02	0.04	70.98	0.01	26	0.09	0.03	0.03	0.02	0.03	13.09	0.01	
3		0.13	0.03	0.03	0.02	0.05	62.53	0.01	27	0.13	0.04	0.03	0.02	0.03	18.25	0.01	
4		0.17	0.03	0.03	0.02	0.05	57.79	0.01	28	0.17	0.04	0.03	0.03	0.03	16.68	0.01	
5		0.19	0.03	0.03	0.02	0.05	57.34	0.01	29	0.19	0.04	0.03	0.03	0.03	17.07	0.01	
6		0.20	0.03	0.03	0.02	0.05	57.34	0.01	30	0.20	0.04	0.03	0.03	0.03	17.04	0.01	
7	0.005	0.05	0.03	0.03	0.01	0.03	41.74	0.01	31	0.07	0.05	0.04	0.03	0.03	23.65	0.01	
8		0.09	0.03	0.03	0.01	0.04	52.63	0.01	32	0.09	0.04	0.03	0.03	0.03	24.57	0.01	
9		0.13	0.03	0.03	0.01	0.04	49.64	0.01	33	0.13	0.04	0.03	0.03	0.03	23.70	0.01	
10		0.17	0.03	0.03	0.01	0.04	44.97	0.01	34	0.17	0.04	0.03	0.04	0.04	41.76	0.01	
11		0.19	0.03	0.03	0.01	0.04	43.63	0.01	35	0.19	0.04	0.03	0.04	0.07	55.41	0.01	
12		0.20	0.03	0.03	0.01	0.04	43.63	0.01	36	0.20	0.04	0.03	0.04	0.07	50.53	0.01	
13	0.01	0.05	0.03	0.03	0.01	0.02	11.61	0.01	37	0.10	0.05	0.04	0.03	0.06	64.42	0.02	
14		0.09	0.03	0.03	0.01	0.02	13.99	0.01	38	0.09	0.04	0.03	0.06	0.25	57.28	0.02	
15		0.13	0.03	0.03	0.01	0.02	14.80	0.01	39	0.13	0.04	0.03	0.06	0.24	55.05	0.02	
16		0.17	0.03	0.03	0.01	0.02	13.86	0.01	40	0.17	0.04	0.03	0.06	0.24	55.05	0.02	
17		0.19	0.03	0.03	0.01	0.02	13.86	0.01	41	0.19	0.04	0.03	0.06	0.31	60.95	0.02	
18		0.20	0.03	0.03	0.01	0.02	13.86	0.01	42	0.20	0.04	0.03	0.07	0.29	61.35	0.02	
19	0.03	0.05	0.03	0.03	0.01	0.03	9.27	0.01	43	0.13	0.05	0.04	0.03	0.09	1.42	104.70	0.02
20		0.09	0.03	0.03	0.01	0.03	10.96	0.01	44	0.09	0.04	0.03	0.09	1.73	116.24	0.03	
21		0.13	0.03	0.03	0.01	0.03	10.20	0.01	45	0.13	0.04	0.03	0.09	$14x10^{100}$	114.39	$13x10^5$	
22		0.17	0.03	0.03	0.01	0.03	10.37	0.01	46	0.17	0.04	0.03	0.09	$14x10^{100}$	127.19	$14x10^{10}$	
23		0.19	0.03	0.03	0.01	0.03	10.30	0.01	47	0.19	0.04	0.03	0.09	$14x10^{100}$	125.52	$14x10^{10}$	
24		0.20	0.03	0.03	0.01	0.03	10.30	0.01	48	0.20	0.04	0.03	0.09	$14x10^{100}$	127.19	$14x10^{10}$	



Table S.8: Nominal coverage, in %, and MSE for the response variable calculated for each mesh with  $b=0.3$ , considering 200 simulations, for  $n=50$ .

Mesh	c	a	Coverage(%)	MSE	Mesh	c	a	Coverage(%)	MSE
1	0.001	0.05	3.51	0.29	25	0.05	0.05	65.38	0.24
2		0.09	3.94	0.29	26		0.09	60.46	0.25
3		0.13	3.97	0.29	27		0.13	82.89	0.24
4		0.17	3.87	0.29	28		0.17	85.77	0.24
5		0.19	4.01	0.29	29		0.19	87.82	0.24
6		0.20	3.89	0.29	30		0.20	87.87	0.24
7	0.005	0.05	3.51	0.29	31	0.07	0.05	85.83	0.25
8		0.09	3.94	0.29	32		0.09	84.81	0.25
9		0.13	3.97	0.29	33		0.13	85.66	0.25
10		0.17	3.87	0.29	34		0.17	87.21	0.26
11		0.19	4.01	0.29	35		0.19	87.00	0.27
12		0.20	3.89	0.29	36		0.20	86.58	0.27
13	0.01	0.05	10.24	0.29	37	0.10	0.05	84.71	0.29
14		0.09	11.66	0.29	38		0.09	84.74	0.29
15		0.13	13.62	0.29	39		0.13	84.91	0.29
16		0.17	13.73	0.29	40		0.17	84.86	0.29
17		0.19	14.01	0.29	41		0.19	84.76	0.29
18		0.20	13.75	0.29	42		0.20	84.72	0.29
19	0.03	0.05	30.92	0.27	43	0.13	0.05	79.78	0.33
20		0.09	46.52	0.26	44		0.09	79.43	0.34
21		0.13	70.26	0.24	45		0.13	78.93	0.34
22		0.17	71.48	0.24	46		0.17	78.92	0.34
23		0.19	74.28	0.24	47		0.19	79.26	0.34
24		0.20	74.16	0.24	48		0.20	79.01	0.34

Table S.9: Nominal coverage, in %, and MSE for the response variable calculated for each mesh with  $b=0.3$ , considering 200 simulations, for  $n=300$ .

Mesh	c	a	Coverage(%)	MSE	Mesh	c	a	Coverage(%)	MSE
1	0.001	0.05	90.08	0.16	25	0.05	0.05	87.74	0.18
2		0.09	86.75	0.17	26		0.09	87.73	0.18
3		0.13	86.99	0.17	27		0.13	84.80	0.19
4		0.17	87.46	0.17	28		0.17	83.81	0.20
5		0.19	87.53	0.17	29		0.19	83.75	0.20
6		0.20	87.53	0.17	30		0.20	83.73	0.20
7	0.005	0.05	90.83	0.16	31	0.07	0.05	81.81	0.21
8		0.09	89.17	0.17	32		0.09	81.69	0.21
9		0.13	88.77	0.17	33		0.13	81.75	0.21
10		0.17	89.53	0.17	34		0.17	78.25	0.22
11		0.19	89.70	0.17	35		0.19	77.31	0.23
12		0.20	89.70	0.17	36		0.20	77.15	0.23
13	0.01	0.05	93.70	0.15	37	0.10	0.05	71.87	0.25
14		0.09	93.42	0.15	38		0.09	71.23	0.26
15		0.13	93.47	0.15	39		0.13	71.49	0.26
16		0.17	93.50	0.15	40		0.17	71.49	0.26
17		0.19	93.49	0.15	41		0.19	71.33	0.26
18		0.20	93.49	0.15	42		0.20	70.73	0.26
19	0.03	0.05	92.30	0.16	43	0.13	0.05	63.44	0.30
20		0.09	90.70	0.16	44		0.09	62.91	0.30
21		0.13	90.06	0.17	45		0.13	62.76	0.30
22		0.17	89.88	0.17	46		0.17	62.47	0.30
23		0.19	89.87	0.17	47		0.19	62.59	0.30
24		0.20	89.87	0.17	48		0.20	62.47	0.30

Table S.10: Nominal coverage, in %, and MSE for the response variable calculated for each mesh with  $b = 0.3$ , considering 200 simulations, for 13 locations not in the analysis, with  $n=50$ .

Mesh	c	a	Coverage(%)	MSE	Mesh	c	a	Coverage(%)	MSE
1	0.001	0.05	93.27	0.54	25	0.05	0.05	84.08	0.57
2		0.09	88.04	0.54	26		0.09	84.42	0.57
3		0.13	79.15	0.54	27		0.13	81.00	0.54
4		0.17	72.12	0.55	28		0.17	75.54	0.54
5		0.19	69.31	0.56	29		0.19	75.00	0.53
6		0.20	65.96	0.56	30		0.20	73.50	0.54
7	0.005	0.05	93.27	0.54	31	0.07	0.05	79.77	0.54
8		0.09	88.04	0.54	32		0.09	79.35	0.54
9		0.13	79.15	0.54	33		0.13	79.15	0.54
10		0.17	72.12	0.55	34		0.17	76.38	0.54
11		0.19	69.31	0.56	35		0.19	75.00	0.54
12		0.20	65.96	0.56	36		0.20	73.73	0.54
13	0.01	0.05	92.62	0.54	37	0.10	0.05	74.38	0.54
14		0.09	87.46	0.54	38		0.09	74.58	0.55
15		0.13	78.62	0.55	39		0.13	74.62	0.54
16		0.17	72.15	0.56	40		0.17	74.54	0.54
17		0.19	69.04	0.56	41		0.19	74.65	0.54
18		0.20	66.19	0.56	42		0.20	74.38	0.54
19	0.03	0.05	90.54	0.55	43	0.13	0.05	71.31	0.54
20		0.09	84.65	0.57	44		0.09	70.92	0.55
21		0.13	80.85	0.54	45		0.13	70.62	0.55
22		0.17	75.42	0.54	46		0.17	70.65	0.55
23		0.19	73.46	0.54	47		0.19	70.81	0.55
24		0.20	71.88	0.54	48		0.20	70.77	0.55

Table S.11: Nominal coverage, in %, and MSE for the response variable calculated for each mesh with  $b = 0.3$ , considering 200 simulations, for 75 locations not in the analysis, for  $n = 300$ .

Mesh	c	a	Coverage(%)	MSE	Mesh	c	a	Coverage(%)	MSE
1	0.001	0.05	87.41	0.31	25	0.05	0.05	79.54	0.30
2		0.09	76.05	0.32	26		0.09	79.50	0.30
3		0.13	73.03	0.32	27		0.13	74.19	0.31
4		0.17	73.11	0.32	28		0.17	70.81	0.31
5		0.19	73.03	0.32	29		0.19	70.17	0.31
6		0.20	73.03	0.32	30		0.20	70.12	0.31
7	0.005	0.05	87.45	0.30	31	0.07	0.05	74.32	0.32
8		0.09	80.17	0.31	32		0.09	74.18	0.32
9		0.13	77.83	0.31	33		0.13	74.26	0.32
10		0.17	77.15	0.31	34		0.17	69.95	0.32
11		0.19	77.11	0.31	35		0.19	67.43	0.33
12		0.20	77.11	0.31	36		0.20	66.99	0.33
13	0.01	0.05	87.60	0.30	37	0.10	0.05	65.80	0.34
14		0.09	81.55	0.30	38		0.09	65.20	0.35
15		0.13	79.32	0.30	39		0.13	65.53	0.34
16		0.17	78.88	0.30	40		0.17	65.53	0.34
17		0.19	78.85	0.30	41		0.19	65.38	0.35
18		0.20	78.85	0.30	42		0.20	64.92	0.35
19	0.03	0.05	86.01	0.30	43	0.13	0.05	58.07	0.37
20		0.09	80.59	0.30	44		0.09	57.44	0.38
21		0.13	75.27	0.30	45		0.13	57.19	0.38
22		0.17	73.94	0.30	46		0.17	56.89	0.38
23		0.19	73.82	0.30	47		0.19	56.73	0.38
24		0.20	73.78	0.30	48		0.20	56.89	0.38

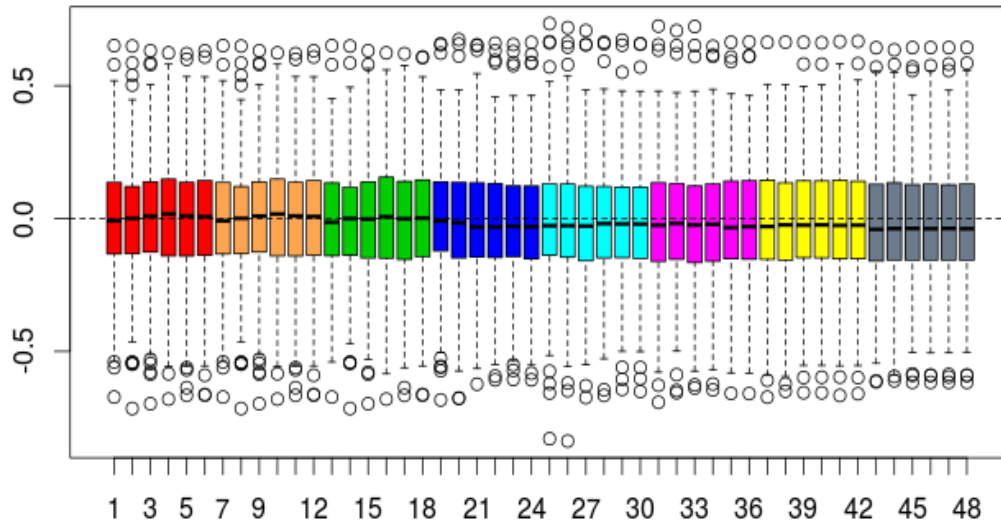


Figure S.4: Bias for the response variable in 13 extra locations, for all 200 simulations, for  $b=0.3$ , considering  $n=50$ .

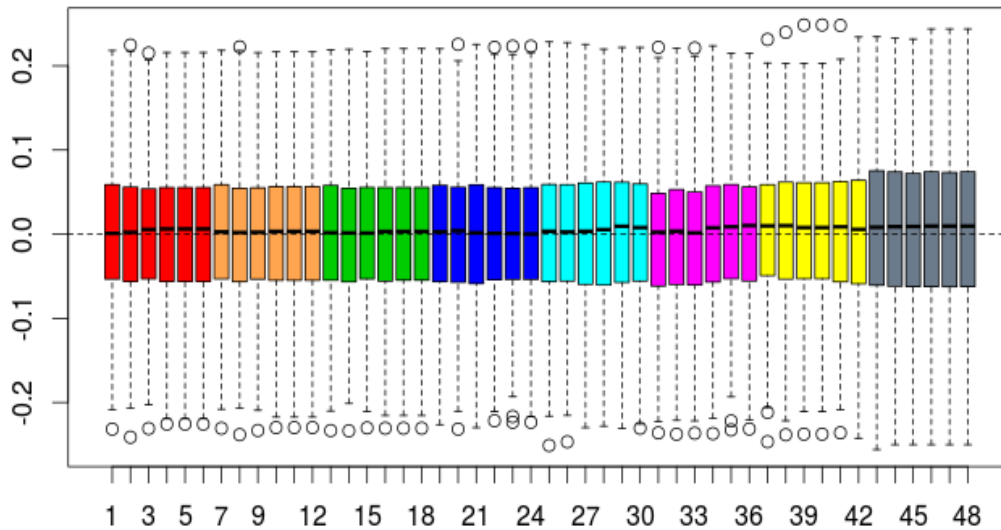


Figure S.5: Bias for the response variable in 75 extra locations, for all 200 simulations, for  $b=0.3$ , considering  $n = 300$ .

### Selecting the best mesh

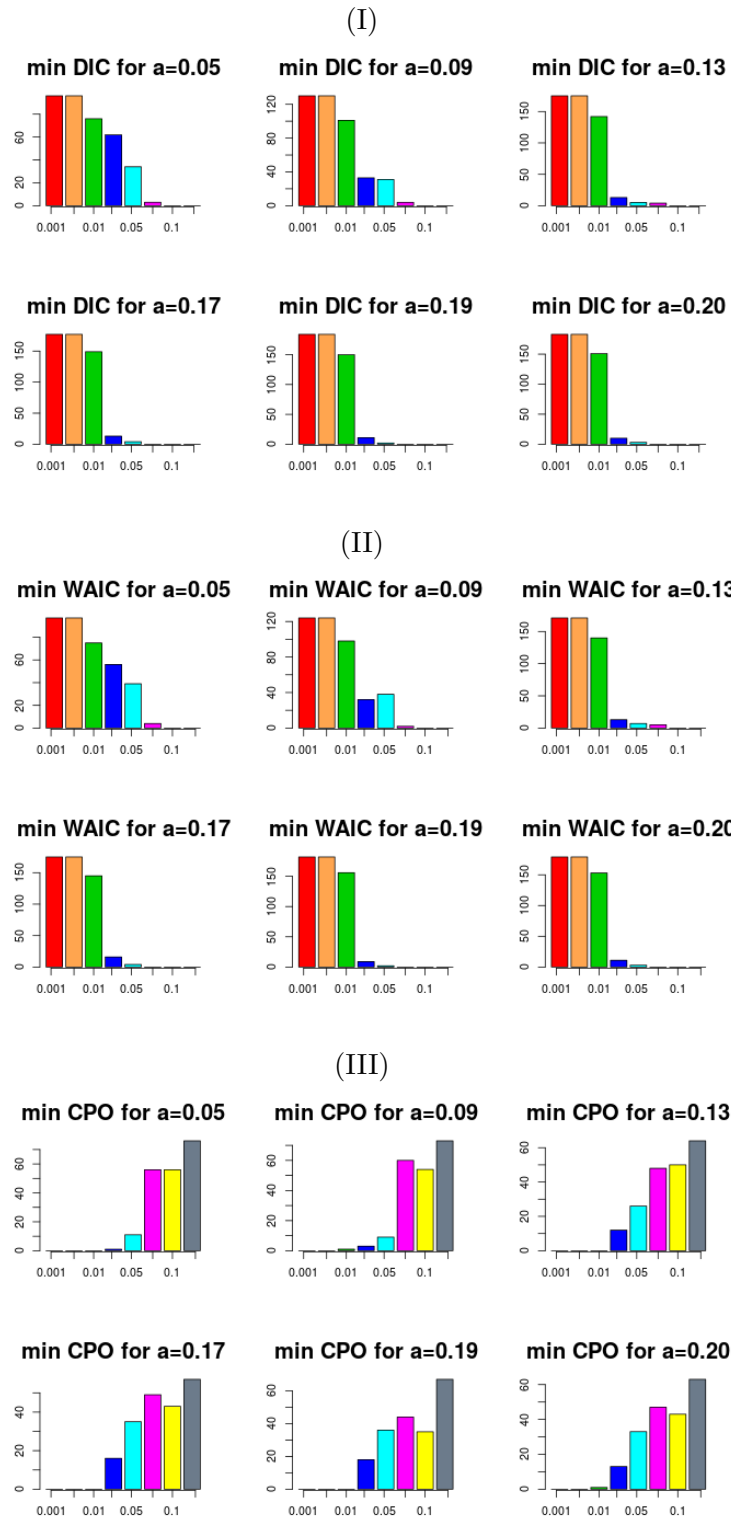


Figure S.6: For each value of  $a$ , minimum value of:(I)DIC; (II) WAIC and (III)logCPO, for all 200 simulations, for  $b=0.3$  with  $n=50$ .

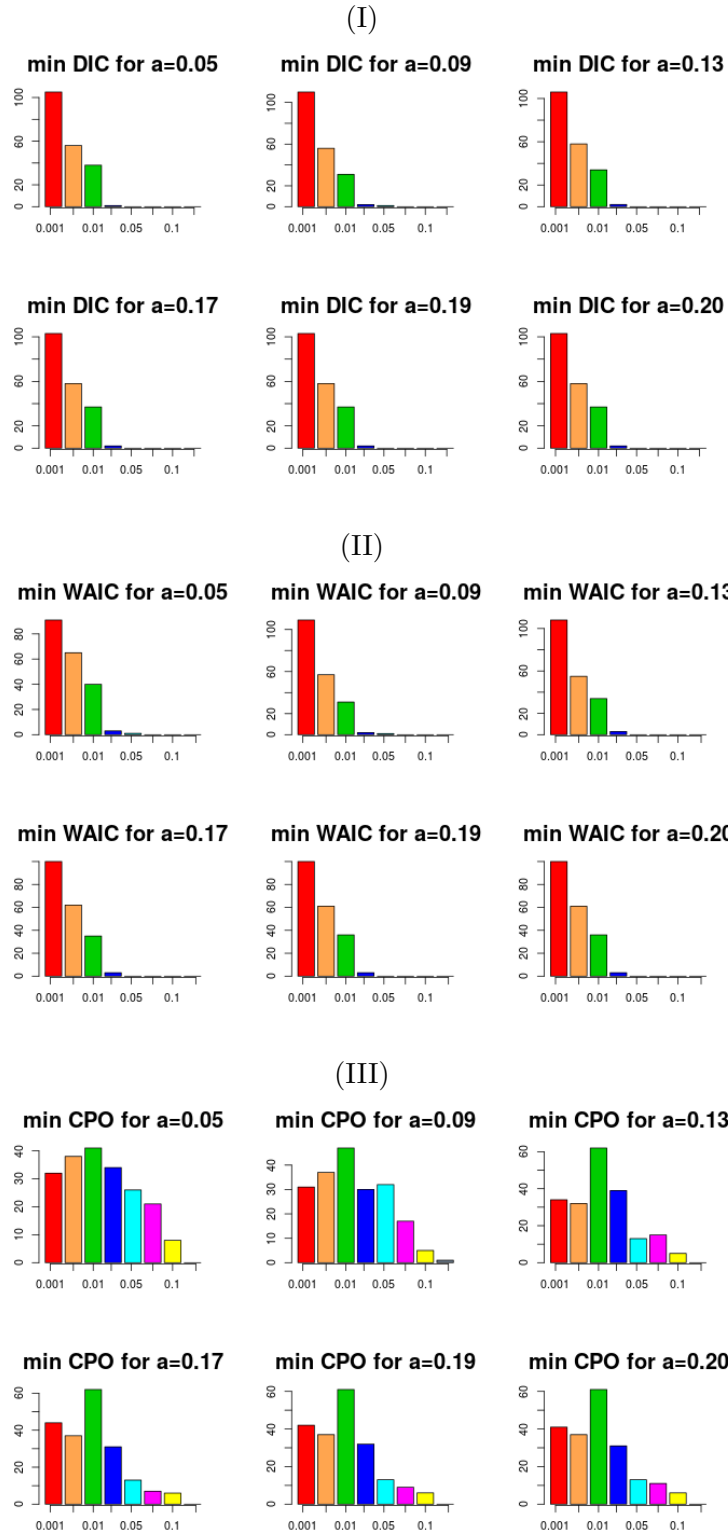


Figure S.7: For each value of  $a$ , minimum value of:(I)DIC; (II) WAIC and (III)logCPO, for all 200 simulations, for  $b=0.3$  with  $n=300$ .

Table S.12: Mean values of DIC, WAIC and logCPO for meshes with  $b=0.3$  for  $n=50$ .

Mesh	c	a	DIC	WAIC	logCPO	Mesh	c	a	DIC	WAIC	logCPO
1	0.001	0.05	-288.32	-295.62	2.31	25	0.05	0.05	-9.21	-5.38	1.69
2		0.09	-286.83	-294.16	2.30	26		0.09	-26.82	-25.34	1.74
3		0.13	-286.75	-293.89	2.26	27		0.13	82.06	84.10	1.43
4		0.17	-286.63	-293.64	2.24	28		0.17	97.90	98.59	1.41
5		0.19	-286.25	-293.34	2.26	29		0.19	108.68	109.72	1.37
6		0.20	-286.39	-293.46	2.25	30		0.20	108.39	109.89	1.37
7	0.005	0.05	-288.32	-295.62	2.31	31	0.07	0.05	103.82	105.70	1.39
8		0.09	-286.83	-294.16	2.29	32		0.09	103.59	104.93	1.39
9		0.13	-286.75	-293.89	2.26	33		0.13	104.92	106.40	1.38
10		0.17	-286.63	-293.64	2.24	34		0.17	119.19	120.30	1.35
11		0.19	-286.25	-293.34	2.26	35		0.19	123.92	124.77	1.35
12		0.20	-286.39	-293.46	2.25	36		0.20	124.63	125.44	1.35
13	0.01	0.05	-259.84	-264.27	2.25	37	0.10	0.05	125.45	126.37	1.35
14		0.09	-253.27	-258.52	2.23	38		0.09	126.95	128.03	1.35
15		0.13	-244.01	-246.87	2.16	39		0.13	127.08	128.03	1.35
16		0.17	-244.53	-245.40	2.12	40		0.17	127.17	128.13	1.35
17		0.19	-242.69	-244.77	2.15	41		0.19	127.35	128.31	1.35
18		0.20	-243.27	-244.81	2.14	42		0.20	127.50	128.45	1.35
19	0.03	0.05	-167.43	-166.10	2.02	43	0.13	0.05	130.57	131.41	1.36
20		0.09	-94.18	-92.02	1.86	44		0.09	131.11	131.95	1.36
21		0.13	14.21	21.02	1.55	45		0.13	131.26	132.08	1.36
22		0.17	24.51	26.20	1.55	46		0.17	131.31	132.14	1.36
23		0.19	36.91	40.09	1.51	47		0.19	131.12	131.98	1.36
24		0.20	36.69	40.18	1.50	48		0.20	131.28	132.11	1.36



Table S.13: Mean values of DIC, WAIC and logCPO for meshes with b=0.3 for n=300.

Mesh	c	a	DIC	WAIC	logCPO	Mesh	c	a	DIC	WAIC	logCPO
1	0.001	0.05	559.42	558.85	1.18	25	0.05	0.05	683.73	684.27	1.17
2		0.09	499.23	494.29	1.20	26		0.09	683.82	684.36	1.17
3		0.13	502.19	495.79	1.20	27		0.13	691.72	692.03	1.18
4		0.17	506.62	502.02	1.20	28		0.17	694.74	695.01	1.18
5		0.19	507.47	502.82	1.20	29		0.19	694.85	695.13	1.18
6		0.20	507.47	502.82	1.20	30		0.20	694.91	695.19	1.18
7	0.005	0.05	581.58	580.48	1.17	31	0.07	0.05	698.96	699.83	1.18
8		0.09	557.66	552.72	1.17	32		0.09	699.29	700.14	1.18
9		0.13	547.11	541.86	1.18	33		0.13	699.05	699.91	1.18
10		0.17	563.49	557.37	1.17	34		0.17	706.11	706.65	1.19
11		0.19	565.44	559.80	1.17	35		0.19	707.55	707.97	1.19
12		0.20	565.44	559.80	1.17	36		0.20	707.72	708.11	1.19
13	0.01	0.05	633.13	634.15	1.16	37	0.10	0.05	718.08	719.39	1.20
14		0.09	634.34	635.34	1.16	38		0.09	719.85	721.11	1.21
15		0.13	633.61	634.30	1.16	39		0.13	719.30	720.53	1.21
16		0.17	634.02	634.72	1.16	40		0.17	719.30	720.53	1.21
17		0.19	634.02	634.70	1.16	41		0.19	719.64	720.86	1.21
18		0.20	634.02	634.70	1.16	42		0.20	720.88	722.01	1.21
19	0.03	0.05	662.41	662.78	1.17	43	0.13	0.05	732.98	733.78	1.23
20		0.09	672.36	672.62	1.17	44		0.09	733.87	734.63	1.23
21		0.13	675.26	675.52	1.17	45		0.13	734.37	735.14	1.23
22		0.17	675.98	676.28	1.17	46		0.17	735.14	735.81	1.23
23		0.19	675.99	676.29	1.17	47		0.19	735.00	735.69	1.23
24		0.20	676.01	676.31	1.17	48		0.20	735.14	735.81	1.23

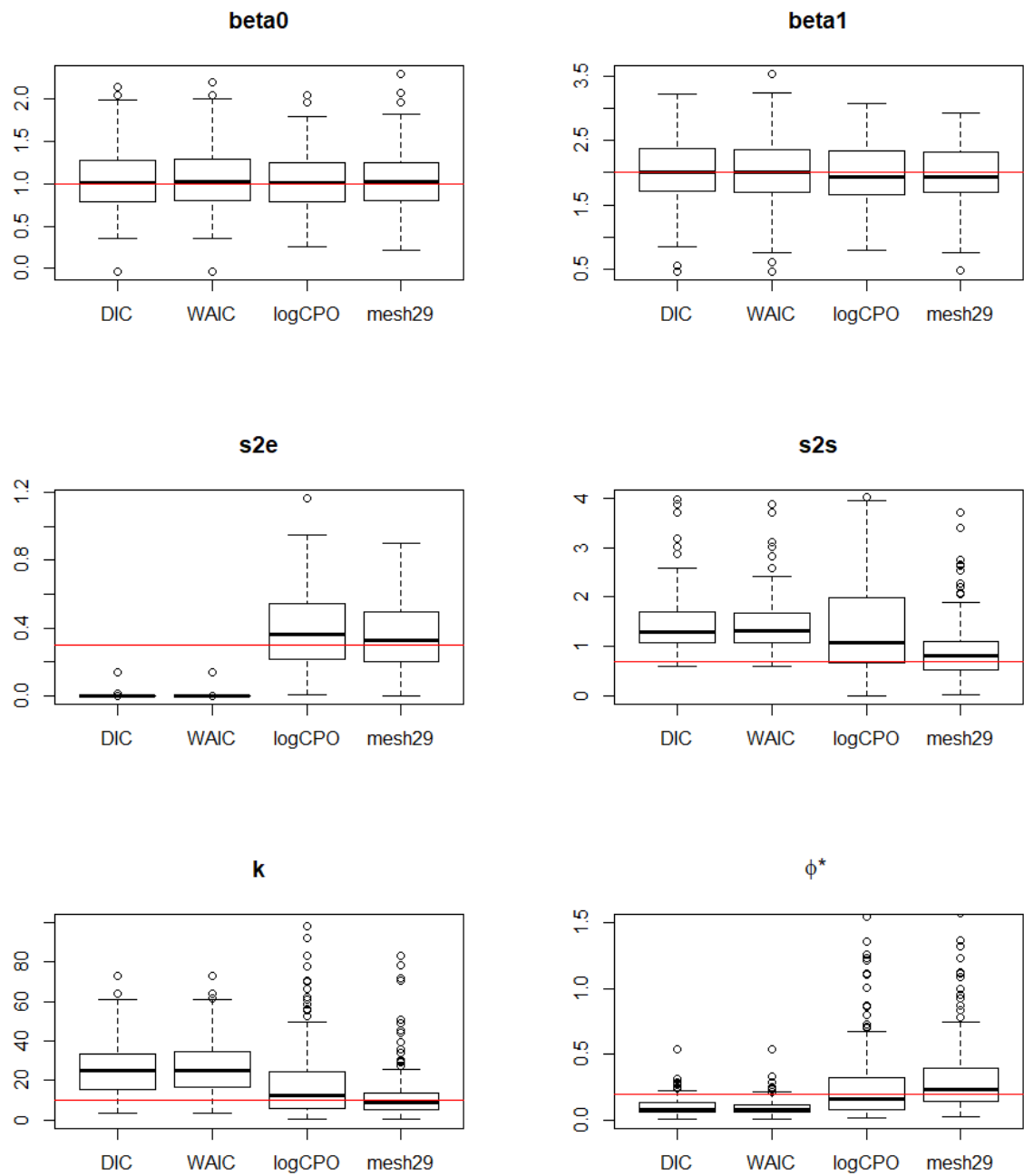


Figure S.8: Estimates for  $\beta_0$ ,  $\beta_1$ ,  $\sigma_e^2$ ,  $\sigma_s^2$ ,  $k$  and  $\phi^*$ , considering the mesh with minimal DIC, WAIC and logCPO, and estimates considering mesh 29, with  $n=50$ .

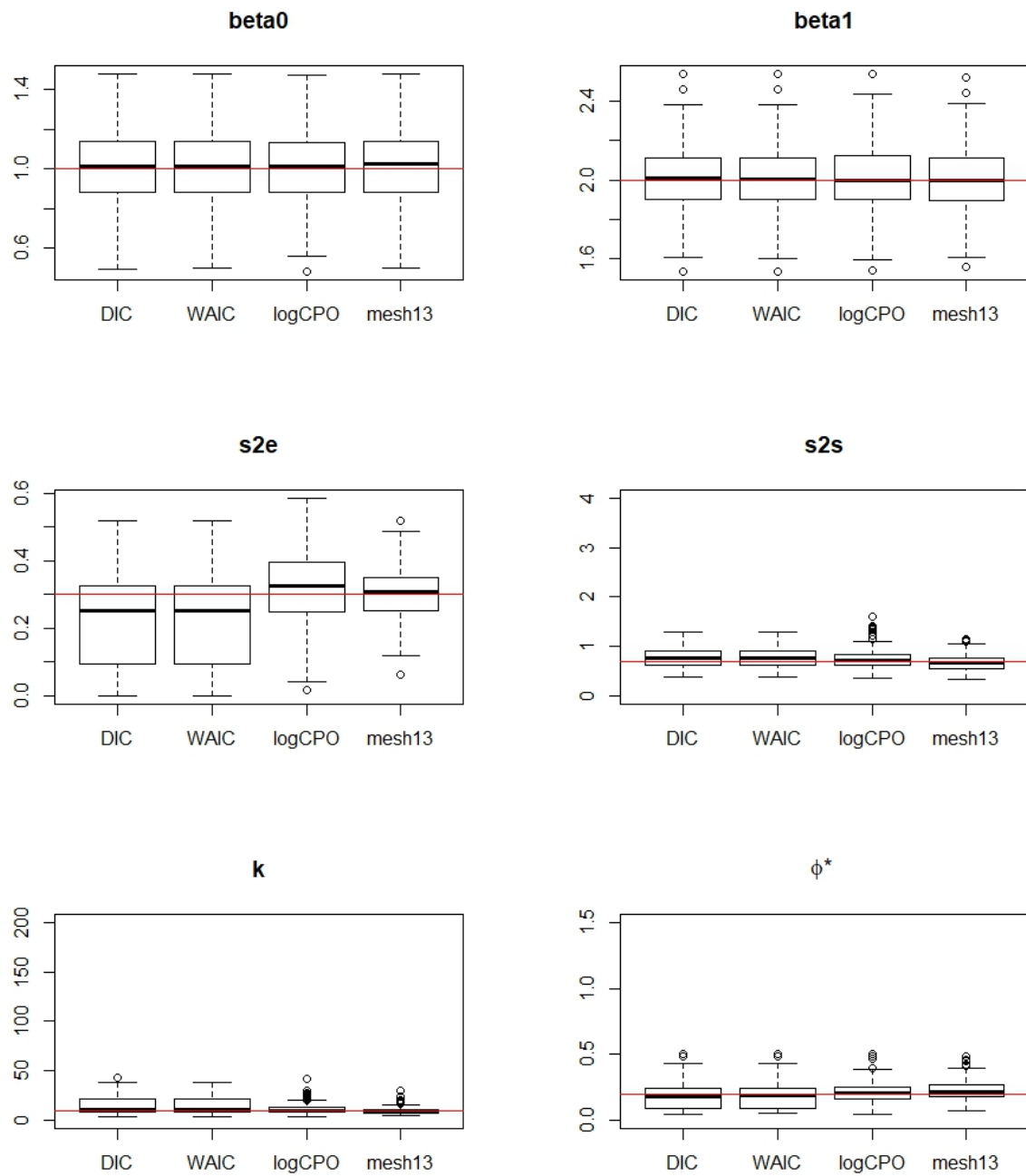


Figure S.9: Boxplots for estimated  $\beta_0$ ,  $\beta_1$ ,  $\sigma_e^2$ ,  $\sigma_s^2$ ,  $k$  and  $\phi^*$ , considering the mesh with minimal DIC, WAIC and logCPO, and boxplots of estimated considering mesh 13, with  $n = 300$ .

## 2 Additional data analysis results

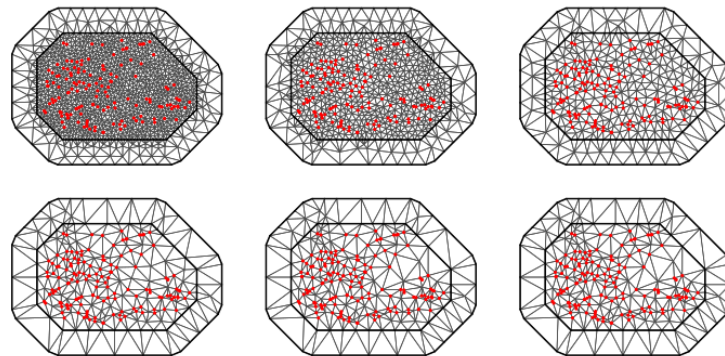


Figure S.10: Meshes with  $c = 13$ ,  $b = 570$  and  $a = (20, 35, 55, 100, 240, 380)$ .

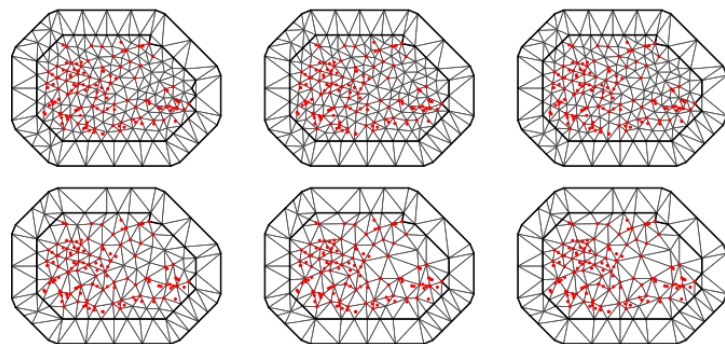


Figure S.11: Meshes with  $c = 35$ ,  $b = 570$  and  $a = (20, 35, 55, 100, 240, 380)$ .

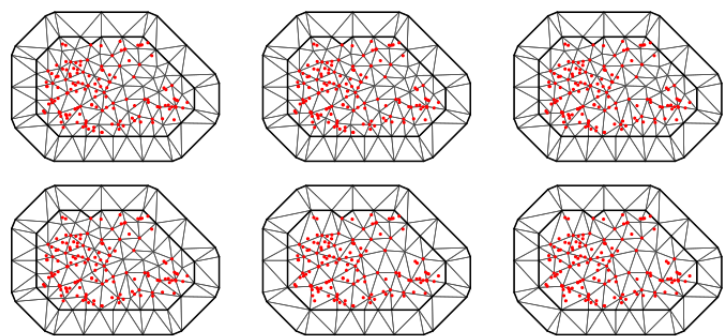


Figure S.12: Meshes with  $c = 51$ ,  $b = 570$  and  $a = (20, 35, 55, 100, 240, 380)$ .

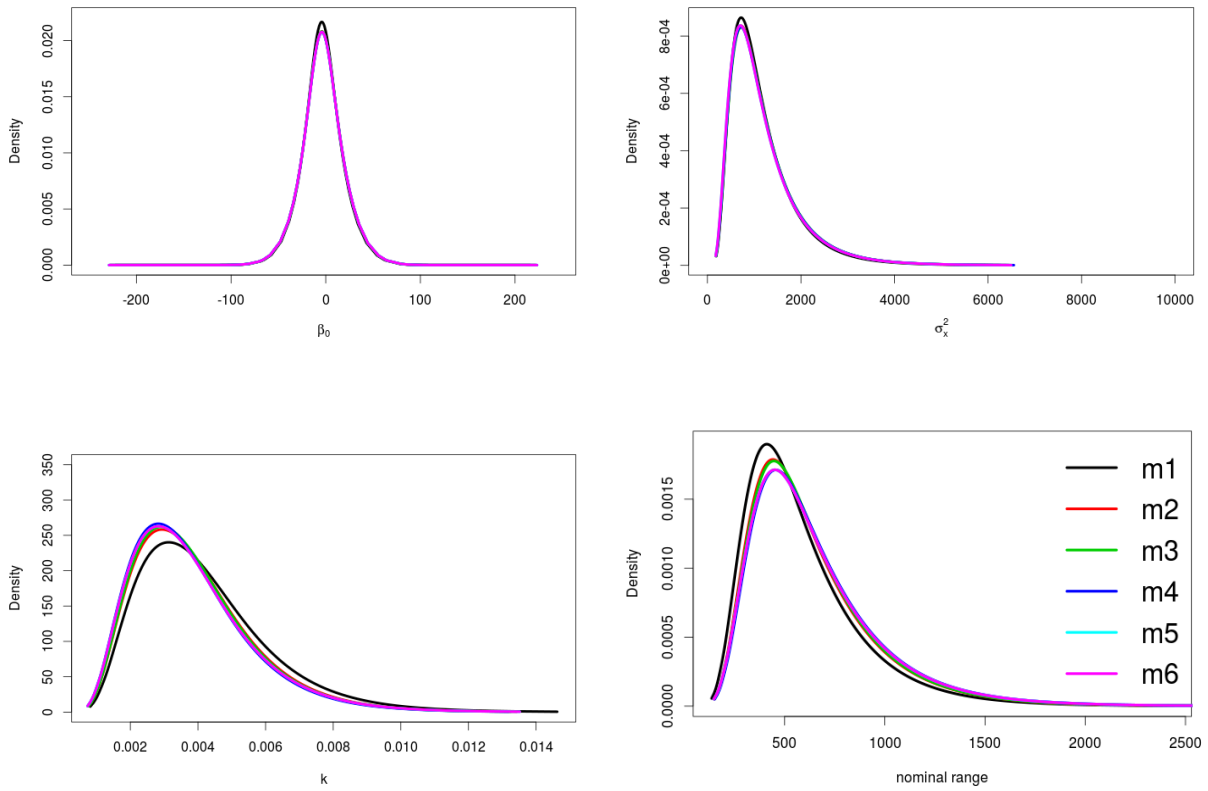


Figure S.13: Posterior density for meshes with  $c = 13$ .

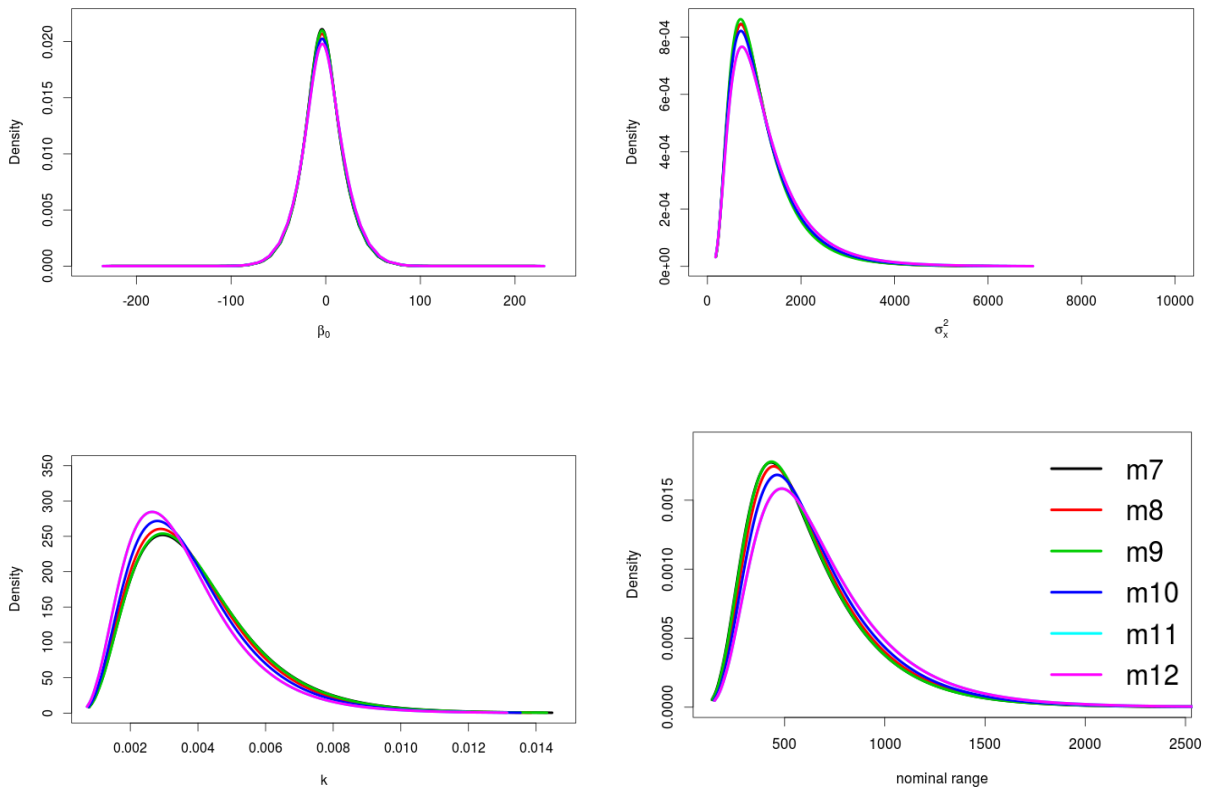


Figure S.14: Posterior density for meshes with  $c = 35$ .

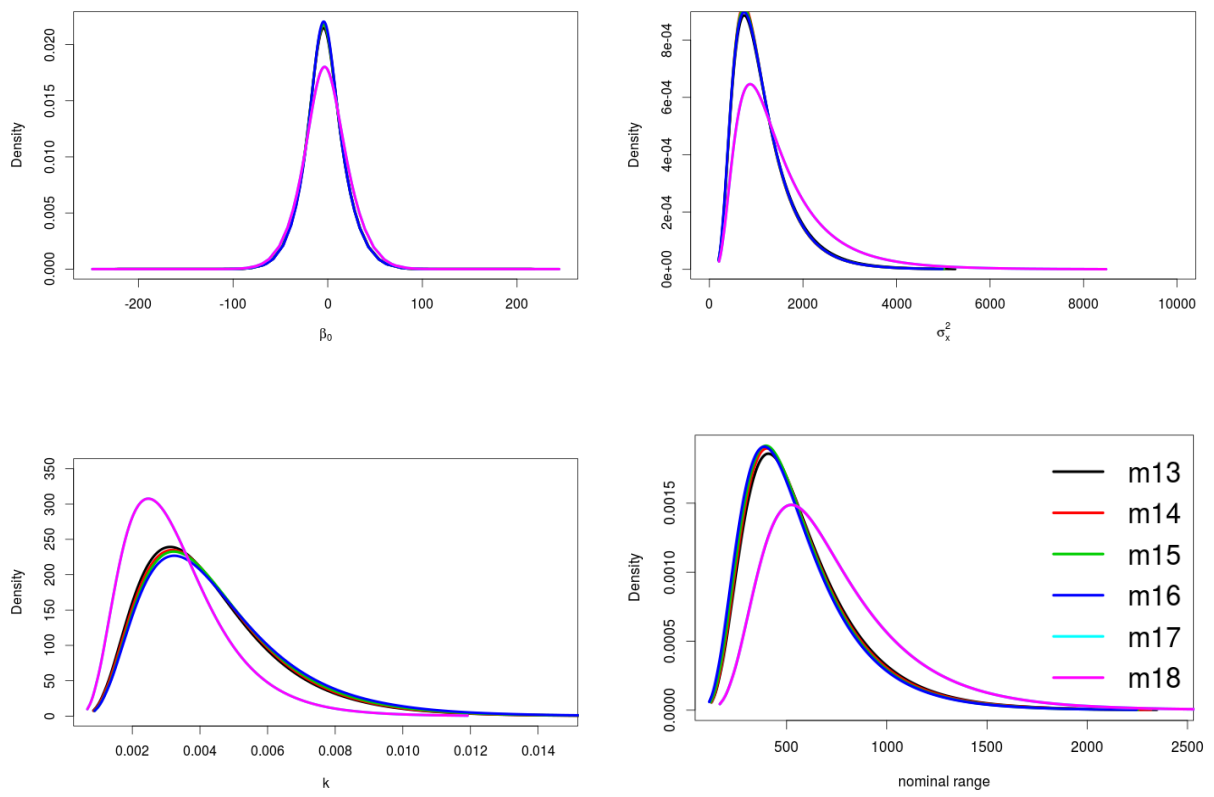


Figure S.15: Posterior density for meshes with  $c = 51$ .